Unravelling the oxygen isotope signal (δ18O) of rodent teeth from northeastern Iberia, and implications for past climate reconstructions.

Mónica Fernández-García, Aurélien Royer, Juan Manuel López-García, Maria Bennàsar, Jean Goedert, François Fourel, Marie-Anne Julien, Sandra Bañuls-Cardona, Antonio Rodríguez-Hidalgo, Josep Vallverdú, et al.

Unravelling the oxygen isotope signal ($\delta^{18}O$) of rodent teeth from northeastern Iberia, and implications for past climate reconstructions

Mónica Fernández-García [a, b, *], Aurélien Royer [c], Juan Manuel López-García [d], Maria Bennàsar [d, e], Jean Goedert [f], François Fourel [g], Marie-Anne Julien [b], Sandra Banuls-Cardona [a], Antonio Rodríguez-Hidalgo [h, i], Josep Vallverdú [d, e], Christophe Lécuyer [j, k]

[a] Sezione di Scienze Preistoriche e Antropologiche, Dipartimento di Studi Umanistici, Università degli Studi di Ferrara (UNIFE), C/ so Ercole I d'Este 32, 44121, Ferrara, Italy
[b] Histoire Naturelle de l'Homme Préhistorique (HNHP, UMR CNRS 7194), Muséum National d'Histoire Naturelle (MNHN), Sorbonne Universités, 1 rue René Panhard, 75013, Paris, France
[c] Biogéosciences, UMR CNRS 6282, Université Bourgogne Franche-Comté, 6 Boulevard Gabriel, 21000, Dijon, France
[d] Institut Català de Paleoecologia Humana i Evolució Social (IPHES), Zona Educacional 4, Campus Sescelades URV (Edifici W3), 43007, Tarragona, Spain
[e] Àrea de Prehistòria, Universitat Rovira i Virgili (URV), Av. Catalunya 35, 43002, Tarragona, Spain
[f] PACEA, UMR CNRS 5199, Université de Bordeaux, Bâtiment B18, Allée Geoffroy Saint-Hilaire, CS 50023, 33615, Pessac, France
[g] Laboratoire d'Ecologie des Hydrosystèmes Naturels et Anthropisés (LEHNA), UMR CNRS 5023, Université Claude Bernard Lyon 1, ENTPE, 69622, Villeurbanne, France
[h] Complutense University, Prehistory, Ancient History and Archaeology Department, 28040, Madrid, Spain
[i] Instituto de Evolución en África (IDEA), C/ Covarrubias 36, 28010, Madrid, Spain
[j] Laboratoire de Géologie de Lyon, UMR CNRS 5276, Université Claude Bernard Lyon 1 and Ecole Normale Supérieure de Lyon, 69622, Villeurbanne, France
[k] Institut Universitaire de France, Paris, France

abstract

Small mammals, especially rodents, constitute valuable proxies for continental Quaternary environments at a regional and local scale. Recent studies have demonstrated the relation between the stable oxygen isotope composition of the biogenic phosphate from rodent teeth ($\delta^{18}O_p$), and the oxygen isotope composition of meteoric waters ($\delta^{18}O_{mw}$), which is related to air temperatures at mid and high latitudes. This work explores the $\delta^{18}O_p$ of rodent tooth enamel (from Murinae and Arvicolinae subfamilies) to investigate the palaeoenvironmental conditions in northeastern Iberia during Marine Isotope Stage 3 (MIS 3; ca. 60-30 ka). Fourteen new $\delta^{18}O_p$ analyses from modern samples in conjunction with forty-six $\delta^{18}O_p$ analyses previously published are used to decipher the isotope record of present-day rodent teeth in this region. Two main factors should be considered in Iberian palaeoenvironmental reconstructions: the singular nature of Iberian $\delta^{18}O_{mw}$ records and the potential seasonality bias of small-mammal accumulation. Methodological proposals are made with a view to ensuring the correct interpretation of the $\delta^{18}O_p$ of small mammals in reconstructing past air temperatures. This methodology is applied to the MIS 3 sequence of the Cova dels Xaragalls site (Vimbodí-Poblet, Tarragona, Spain), where fifty-one $\delta^{18}O$ analyses were performed on wood mouse (Apodemus sylvaticus) lower incisors. A spring-early summer accumulation of small mammals is suggested for the layers at Cova dels Xaragalls. In agree- ment with previous environmental studies of the site, variations in the $\delta^{18}O_p$ values suggest slight fluctuations in the climatic conditions throughout the sequence, which are consistent with the stadial-interstadial alternations that characterized MIS 3. Complementary palaeoenvironmental methods determine cooler conditions than nowadays, but within a globally stable climatic period.

* Corresponding author. Sezione di Scienze Preistoriche e Antropologiche, Dipartimento di Studi Umanistici, Università degli Studi di Ferrara (UNIFE), C/ so Ercole I d'Este 32, 44121, Ferrara, Italy.
E-mail address: frnmnc@unife.it (M. Fernández-García).

1. Introduction

The Iberian Peninsula is located at mid latitudes, with an area of

582,000 km^2 and an average altitude of 660 m. This peninsula constitutes the southwestern extremity of the Eurasian continent, from which it is partially isolated by the Pyrenean Mountains. Today, Iberia experiences temperate climatic conditions, which nonetheless vary spatially due to the proximity of the Atlantic Ocean, the Mediterranean Sea and the Pyrenean Mountains. The specific orography of the Iberian Peninsula adds further complexity by structuring the climate and the landscape, with the Central Meseta located at high altitudes (660 m), surrounded by several ranges such as the Sierra Nevada and the Cantabrian Mountains. The Galician-Cantabrian and Pyrenean mountain systems shelter the rest of the peninsula from the Atlantic Ocean and the continental cold air masses coming from the northwest and the northeast, respectively. The combination of all these factors gives the Iberian Peninsula exceptional environmental conditions in relation to the rest of the Eurasian continent.

The Late Pleistocene glacial regime and subsequent glacial-interglacial fluctuations had an impact both on flora and fauna, including human populations throughout western Europe and the Iberian Peninsula (Uriarte, 2003; Arrizabalaga, 2004). In southern Europe, Marine Isotope Stage 3 (MIS 3; ca. 60-30 ka) was characterized by climate dynamics that alternated between warming and cooling periods of sea-surface temperatures, which on the continent generated phases of forest development and expansion of semi-arid areas, respectively (Fletcher et al., 2010; Harrison and Sanchez Goñi, 2010). However, pollen and small-mammal studies have shown that these alternations are not easily resolved in regional and local contexts, suggesting Iberia never underwent a complete loss of woodland, even during stadials or Heinrich events (Fletcher et al., 2010; López-García et al., 2014). Small-vertebrate assemblages, which reflect local environments, reveal cooler and wetter conditions for MIS 3. It has been observed that the coexistence of cold- and temperate-adapted species varies with the stadial and interstadial fluctuations, although woodland-dwelling species are always frequent (Fernández-García et al., 2016; López-García et al., 2014). The Iberian Peninsula served as a macrorefugium for many floral and faunal species during stadial periods, sheltering them from harsher climatic episodes until more favourable environmental conditions allowed their geographic radiation (Hewitt, 2000; Sommer and Nadachowski, 2006).

To obtain a more complete view of past changes in climate and biodiversity, it is necessary to expand the continental palaeoenvironmental record, which is underrepresented compared to marine and ice-core records. Geochemical approaches based on stable oxygen isotope compositions ($\delta^{18}O$) represent a promising tool for obtaining high-resolution environmental records from regional and local contexts. Isotope compositions measured from mammalian bone and tooth fossils permit the quantification of climatic parameters, due to the interdependence of climatic variables such as air temperatures, the oxygen isotope composition of meteoric waters ($\delta^{18}O_{mw}$) and the oxygen isotope composition of body tissues (Dansgaard, 1964; Kolodny et al., 1983; Longinelli, 1984; Longinelli and Nuti, 1973; Luz et al., 1984; Rozanski et al., 1993). These isotopic data can be combined with palaeoecological data inferred from vertebrate assemblages in order to obtain a coherent and refined picture of continental palaeoenvironments (e.g. Freudenthal et al., 2014; Royer et al., 2013b, 2014). Advances in chemical techniques and analytical methodologies now offer an opportunity to perform geochemical analyses on small-mammal teeth, which are particularly relevant in documenting high-resolution climatic changes at a regional or a local scale (e.g. Barham et al., 2017; Freudenthal et al., 2014; García-Alix, 2015; Grimes et al., 2003; Héran et al., 2010; Jeffrey et al., 2015; Leichliter et al., 2017; Lindars et al., 2001; Navarro et al., 2004).

Unfortunately, interpreting the oxygen isotope composition of small-mammal skeletal apatite is not straightforward, and several questions concerning its application to the fossil record have recently been raised (Barham et al., 2017; Jeffrey et al., 2015; Peneycad et al., 2019; Royer et al., 2014, 2013a, 2013b). The question of prey-predator interactions is considered to be of paramount importance in deciphering the isotopic signal recorded in accumulated fossil rodent remains, especially for regions with a specific climatic mode such as the Iberian Peninsula. The main purpose of this work is thus to develop an isotopic framework for environmental and climatic reconstructions for the Iberian Peninsula, based on the oxygen isotope composition of phosphate ($\delta^{18}O_p$) from present-day rodent teeth recovered from pellets. A first step aims to assess the specific role of the climatic context of the Iberian Peninsula, whilst a second one seeks to achieve a better understanding of $\delta^{18}O$ from small-mammal teeth, focusing on the origin of the remains and their period of production. A refinement of the interpretation of the $\delta^{18}O_p$ of fossil rodent tooth phosphate in terms of palaeotemperature reconstructions is finally applied to Cova dels Xaragalls assemblage. This Iberian Late Pleistocene sedimentary sequence, rich in small-vertebrate remains, thus offers the opportunity to reconstruct climate parameters in a continental environment contemporaneous with MIS 3.

2. Cova dels Xaragalls (Tarragona, Spain)

Cova dels Xaragalls is located in Poblet Forest in the municipality of Vimbodí-Poblet (Tarragona), on the left margin of the Castellfollit Creek in the head of the Francolí River basin at 590 m a.s.l. (Fig. 1A). It is a fossiliferous cave of phreatic origin hosted within Mesozoic limestones and Paleozoic schist. The site can be separated into two main areas: a Holocene sequence is developed at the entrance, and at the interior termination of the cave system, in the "Sala Gran" gallery, there is a Pleistocene sequence (Fig. 1B). The fossil remains analysed in this work were recovered from "Sala Gran", a 3 m-thick poorly stratified gravel rich outcrop (scree deposits), during excavations initiated in 2008 (López-García et al., 2012). The deposits that contains the small-vertebrate fossils are typical cave breccia derived from outer slope deposits that entered to the cave through fracture opening. Two bed sets were defined in the stratigraphic sequence of "Sala Gran". Unit 2, containing breccia strata C8-C5, is made from infilled clast-supported fine to medium gravels. Gravels shows inverse and normal grading and partly infilled matrix which has sandy mud texture and red yellow color. Unit 2 contains large boulders in the lower strata from early talus slope rock falls. Unit 1, comprising breccia strata C4-C1, is composed of clast-supported fine to medium gravels infilled by granular red yellow sandy mud matrix with a huge quantity of small-vertebrate and charcoal remains. Gravel beds of the Unit 1 shows grading and scoured surfaces related to the fluvial incision of small rills on the surface of the cave entrance deposits (talus cone). Three radiometric dates are available for the site: one charcoal ^{14}C date from layer C6 recorded an outside range result interpreted as an age older than 43,500 years BP; one charcoal ^{14}C AMS date from layer C4 gave an age of 45,120–48,240 cal years BP; and a stalagmite plate from layer C1 dated via U/Th geochronology yielded an age of 13,723 ± 99 years (Vallverdú et al., 2012) (Fig. 1C).

Colder and wetter periods compared to present-day conditions have been reconstructed using both small vertebrates and charcoal from the site (López-García et al., 2012). Indeed, the regular presence of woodland-dwelling species, including the notable abundance of the wood mouse (Apodemus sylvaticus), throughout the sequence attests to the surrounding landscape being regularly constituted by open-forest. Although the wood mouse is a generalist species capable of inhabiting forested to shrubby areas, but also crops, meadows, heaths or boundaries, this species has a clear

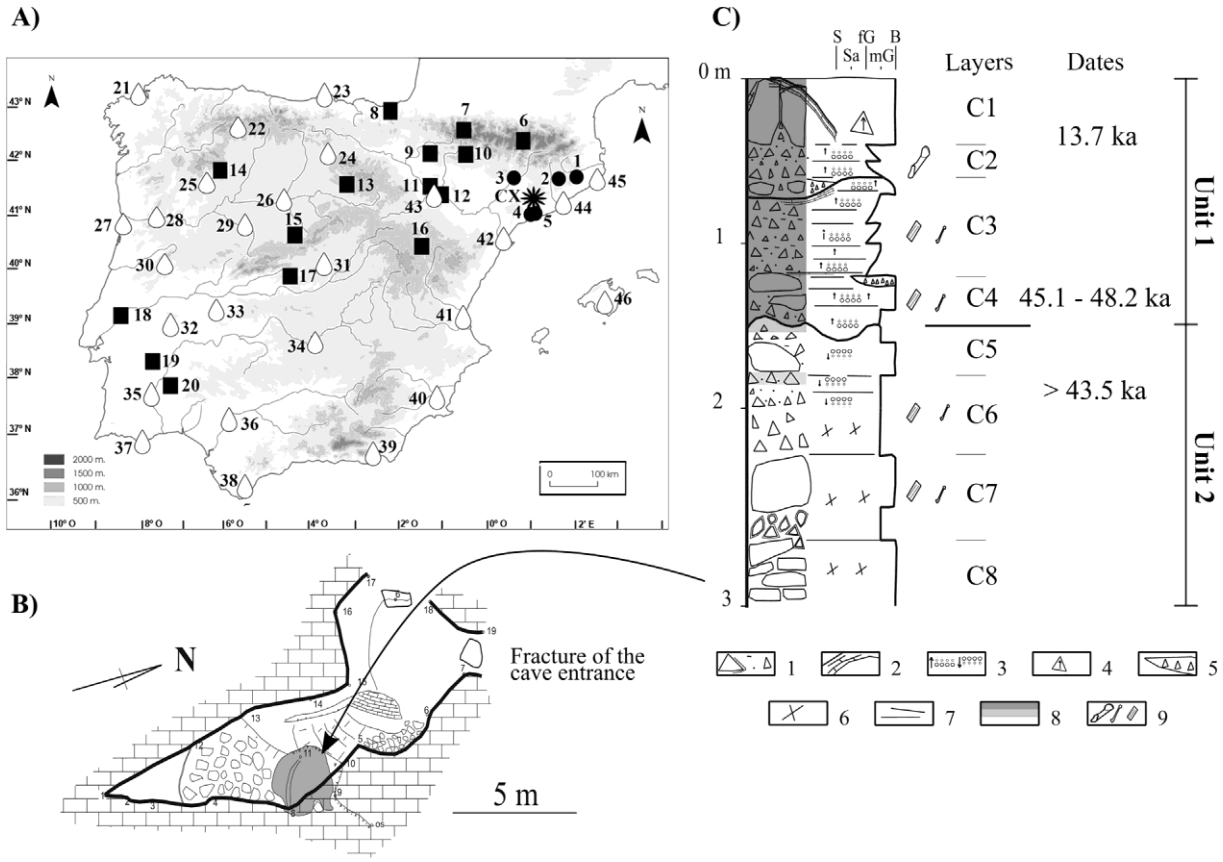

Fig. 1. A) Map showing the location of Cova dels Xaragalls (CX), Iberian localities where present-day oxygen isotope analyses have been performed (black dots, this work; black squares, Royer et al. (2013a)) and IAEA/WMO stations (light grey drops; IAEA/WMO, 2018); 1, Serinyà; 2, Moià; 3, Balaguer; 4, Prades; 5, El Catllar; 6, Espot; 7, Basarán; 8, Berastegui; 9, Uncastillo; 10, Lárrede; 11, Sobradiel; 12, Zaragoza; 13, Palacios de la Sierra; 14, Cernadilla; 15; Yanguas de Eresma; 16, Caminreal; 17, San Martín de Valdeiglesias; 18, Tomar; 19, Redondeo; 20, Amareleja; 21, La Coruna; 22, Leon (Virgen del Camino); 23, Santander; 24, Burgos (Villafría); 25, Braganza; 26; Valladolid; 27, Porto; 28, Vila Real; 29, Salamanca (Matacán); 30, Penhas Douras; 31, Madrid (Retiro); 32, Porto Alegre; 33, Cáceres (Trujillo); 34, Cuidad Real; 35, Beja; 36, Sevilla (Morón Base); 37, Faro; 38, Gibraltar; 39, Almería airport; 40, Murcia; 41, Valencia; 42, Tortosa; 43, Zaragoza airport; 44, Barcelona; 45, Girona airport; 46, Palma de Mallorca. B) Topographic sketch showing the situation of the Sala Gran of Cova dels Xaragalls, with the studied section highlighted in grey. C) Lithostratigraphy of the sampled section in the Sala Gran. Strata number (C1 to C8); II, dates (U-series and cal. BP); III, bedsets (units 1 and 2); S, speleothem; Sa, sands; fG, fine gravels; mG, medium gravels; B, boulder; 1, clastic particles: boulder, gravels, sands and mud; 2, speleothem; 3, normal and inverse grading; 4, vertical boulder; 5: sieve deposit (open work clast supported fine gravels) on scoured surface; 6, disorganized and unstratified strata; 7: horizontal stratification; 8: breccia of open work, party infilled and totally infilled (by sandy mud) clast-supported structure; 9: large-vertebrate, small-vertebrate and charcoal remains.

preference for low-altitude areas with good tree cover, under the influence of a Mediterranean climate, in which it can collect diverse foods (Palomo et al., 2007; Sánchez-González et al., 2016; IUCN, 2018). Layers C8 and C5 correspond to warmer environmental conditions with open dry meadows in contrast to layers C4 and C3, which are interpreted to represent more humid and cooler conditions with landscape openings. The origin of the small-vertebrate remains recovered from the whole sequence was associated with predation. Homogeneity observed among digestion degrees inside each level suggests the activity of a single type of predator. The percentage of incisors, molars and femurs showing signs of digestion and the degree of alteration observed suggest that the predator of layers C4, C6, C7 and C8 would have been a nocturnal bird of prey similar to a little owl (Athene noctua) (López-García et al., 2012). This sedentary predator is an opportunistic hunter that yields a faithful record of the prey originally present in its ecosystem (Andrews, 1990). Thus, changes in both the small-vertebrate compositions and in the relative abundance of the wood mouse can be interpreted as real changes in local ecosystem conditions. According to charcoal studies of this sedimentary sequence, the forest was less taxon-diverse than the current Poblet Forest, with a clear predominance of Pinus-type sylvestris, confirming the harsher conditions during the stage under study. For this sequence, correlations with global climatic fluctuations have been proposed, relating layer C8 to Interstadial 15 or 16 (ca. 56e59 ka), layer C5 to Interstadial 13 or 14 (ca. 50e55 ka) and layers C4-C3 to Heinrich Event 5 (ca. 47 ka) (López-García et al., 2012).

3. Material and methods

3.1. Recovery of small-mammal remains

3.1.1. Modern samples from northeastern Iberia

Fourteen lower incisors from present-day rodents were collected from pellets to analyse their oxygen isotope composition ($\delta^{18}O$). These pellets were collected from five different sites located in northeastern Iberia (Figs. 1A and 2; Table 1): Serinyà (Girona), Moià (Barcelona), Prades (Tarragona), Balaguer (Lleida) and El Catllar (Tarragona). The sites are distributed within the same latitudinal range (from 41° N to 42° N) but at different altitudes ranging from 188 m a.s.l. at Serinyà to 1000 m a.s.l. at Moià (Fig. 1A; Table 1). Northeastern Iberia is mostly assigned a Mediterranean climate. The five selected localities correspond to different climate subtypes from this region, defined considering local factors, such as

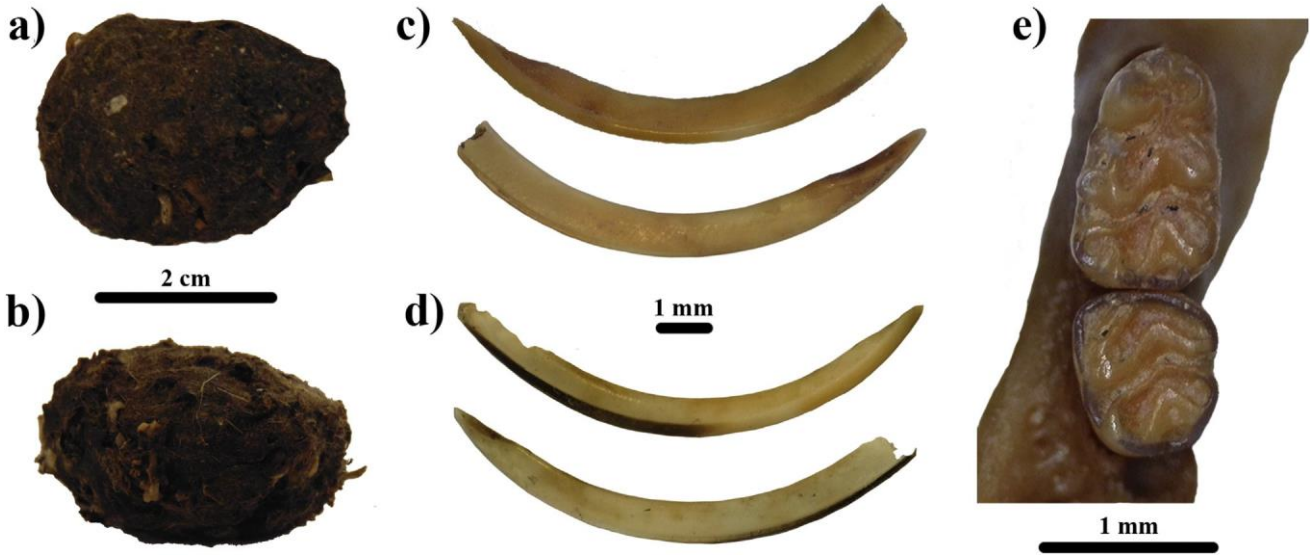

Fig. 2. a) Tyto alba pellet from Serinyà (Girona); b) Tyto alba pellet from Moià (Barcelona); c) left lower incisor of Apodemus sylvaticus from Cova dels Xaragalls, in labial and lingual view; d) right lower incisor of Apodemus sylvaticus from a pellet from Serinyà, in labial and lingual view; e) left mandible with m1 and m2 of Apodemus sylvaticus from Cova dels Xaragalls, in occlusal view.

Table 1
Oxygen isotope composition of tooth enamel phosphate ($\delta^{18}O_p$; ‰ V-SMOW) from present-day rodent lower incisors. The table includes information about the pellet, the location where it was recovered and identified taxa. SD, Standard Deviation.

Sample	Location	Coordinates	Altitude (m)	Climatic subtype	MAT (°C)	MAP (mm)	Predator	Recovering	Taxon	Laterality	$\delta^{18}O_p$	SD
MA-3	Serinyà	42° 10′ 7″ N; 2° 47′ 42″ E	188	Northern pre-littoral	14.8	733	Tyto alba	August–September	Microtus (T.) duodecimcostatus	left	18.8	0.4
MA-1	Serinyà	42° 10′ 7″ N; 2° 47′ 42″ E	188	Northern pre-littoral	14.8	733	Tyto alba	August–September	Apodemus sylvaticus	right	19.0	0.1
MA-2	Serinyà	42° 10′ 7″ N; 2° 47′ 42″ E	188	Northern pre-littoral	14.8	733	Tyto alba	August–September	Apodemus sylvaticus	left	19.5	0.3
MA-12	Moià	41° 48′ 51″ N; 2° 11′ 54″ E	1000	Continetal sub-humid	12.3	749	Tyto alba	Unknown	Microtus (T.) duodecimcostatus	right	16.1	0.4
MA-4	Moià	41° 48′ 51″ N; 2° 11′ 54″ E	1000	Continetal sub-humid	12.3	749	Tyto alba	End of August	Microtus (T.) duodecimcostatus	left	18.6	0.4
MA-6	Moià	41° 48′ 51″ N; 2° 11′ 54″ E	1000	Continetal sub-humid	12.3	749	Tyto alba	End of August	Mus musculus	right	19.2	0.3
MA-5	Moià	41° 48′ 51″ N; 2° 11′ 54″ E	1000	Continetal sub-humid	12.3	749	Tyto alba	End of August	Mus musculus	left	19.5	0.3
MA-14	Balaguer	41° 45′ 21″ N; 0° 47′ 25″ E	200	Continental dry	14.3	501	Tyto alba	Unknown	Microtus (T.) duodecimcostatus	right	17.4	0.3
MA-13	Balaguer	41° 45′ 21″ N; 0° 47′ 25″ E	200	Continental dry	14.3	501	Tyto alba	Unknown	Microtus (T.) duodecimcostatus	left	18.9	0.1
MA-9	Prades	41° 18′ 35″ N; 0° 59′ 19″ E	990	South pre-littoral	12.6	728	Strix aluco	September	Apodemus sylvaticus	left	18.3	0.4
MA-10	Prades	41° 18′ 35″ N; 0° 59′ 19″ E	990	South pre-littoral	12.6	728	Strix aluco	September	Apodemus sylvaticus	left	19.5	0.6
MA-11	Prades	41° 18′ 35″ N; 0° 59′ 19″ E	990	South pre-littoral	12.6	728	Strix aluco	September	Apodemus sylvaticus	right	20.2	0.4
MA-7	El Catllar	41° 11′ 5″ N; 1° 20′ 14″ E	110	Southern littoral	15.9	562	Tyto alba	Unknown	Mus musculus	right	18.2	0.2
MA-8	El Catllar	41° 11′ 5″ N; 1° 20′ 14″ E	110	Southern littoral	15.9	562	Tyto alba	Unknown	Mus musculus	left	18.8	0.4

continentality or orography (Font-Tullot, 2000; Meteocat, 2018).

The teeth recovered belong to three extant species of the Muroidea superfamily: the wood mouse (Apodemus sylvaticus), the Mediterranean pine vole (Microtus (Terricola) duodecimcostatus) and the house mouse (Mus musculus). The teeth were extracted from owl pellets from nest or roosting sites (Fig. 2). The pellets were recovered in August–September in fresh (Serinyà) or semi-dry (Moià and Prades) states. However, pellets can be preserved over several months depending on their exposure to weather conditions. These pellets were produced by either the barn owl (Tyto alba) or the tawny owl (Strix aluco). Both are opportunistic hunters, sedentary and highly territorial species, nesting in tree holes, cliffs or buildings that are reused year after year. Their hunting area ranges from 3 to 10 km^2 for T. alba and is less than 3 km^2 for S. aluco (Mikkola, 1983; Yalden, 2009; IUCN, 2018).

3.1.2. Fossil samples from Cova dels Xaragalls

The rodent remains from Cova dels Xaragalls were collected by

water-screening using superimposed 5 and 0.5 mm mesh sieves and then sorted at the Institut Català de Paleoecologia Humana i Evolució Social (Tarragona). The specific attribution of the remains and the taphonomic study were performed by López-García et al. (2012). Oxygen isotope compositions were measured on 46 teeth from layers C8 to C4. To avoid possible interspecies variability, A. sylvaticus fossil incisors were preferentially selected, with 44 incisors representing at least 29 individuals (Fig. 2). One tooth from Microtus arvalis and one tooth from Eliomys quercinus were also included (Table 2). Taking into account previous works (Lindars et al., 2001; Navarro et al., 2004; Royer et al., 2013a), a minimum five to ten samples were selected from each layer in order to analyse a representative population.

3.2. Sampling procedure for oxygen isotope analysis

For each rodent sample, only lower incisor enamel was sampled, as the mineral fraction is greater in tooth enamel than in dentine or bones, favouring preservation of the original isotopic composition (Barham et al., 2017; Kolodny et al., 1983; Lécuyer et al., 1999; Lee-Thorp and van der Merwe, 1991; Zazzo et al., 2004). Unbroken and well-preserved lower incisors were preferentially selected, whereas remains with physical damage such as soil or root corrosion, manganese oxide coatings, fissures and cracks, cementation or water abrasion, which could facilitate diagenetic alteration of the oxygen isotopic system, were systematically avoided (Andrews, 1990; Barham et al., 2017; Royer et al., 2014). In addition, all rodent remains showing clear evidence of digestion were discarded due to the possible modification of the original oxygen isotope composition that may result from the chemically and enzymatically digestive environment (Barham et al., 2017), and incisors preserved inside the mandible were preferred because they were likely to be more protected from chemical exchange with sedimentary matrices (Royer et al., 2013b). Only adult specimens were selected, to avoid the possible damping of the oxygen isotope composition associated with the immature teeth of juvenile individuals, where the mineralization process is incomplete (Blumenthal et al., 2014; Passey and Cerling, 2002).

The phosphate radical (PO_4^{3-}) constitutes the major source of oxygen in biogenic apatite, and the phosphorus-oxygen bond is stronger than the carbon-oxygen one (CO_3^{2-}), and less prone to geochemical and biological alteration (Clementz, 2012; Grimes et al., 2008; Lécuyer et al., 1999; Lindars et al., 2001). Pristine oxygen isotope compositions can thus be preserved over geological timescales even though the diagenetic alteration of biogenic apatite cannot be excluded in some cases, such as during processes of dissolution and recrystallization induced by microbial activity (Blake et al., 1997; Zazzo et al., 2004). On the basis of phosphate chemical yields measured during the wet chemistry procedure after described, clustered phosphorus pentoxide (P_2O_5) contents close to 40 wt% indicate that the original stoichiometry of the analysed teeth was most likely preserved (Héran et al., 2010; Lécuyer, 2004; Navarro et al., 2004; Royer et al., 2013b).

3.3. Analytical techniques

The rodent teeth were cleaned with double-deionized water (DDW) in an ultrasonic bath to remove any trace of sediment matrix. Then, the basal part of the enamel was discarded while the remaining part was gently crushed in an agate mortar. Enamel fragments were separated from dentine by hand-picking under a binocular microscope. The enamel tooth samples were treated following the wet chemistry procedure described by Crowson et al. (1991) and slightly modified by Lécuyer et al. (1993) and adapted for small-sample weights (1e3 mg of apatite) by Bernard et al. (2009), Fourel et al. (2011) and Lécuyer et al. (2007). This protocol is based on the isolation of phosphate ions (PO_4^{3-}) from apatite as trisilver phosphate (Ag_3PO_4) crystals using acid dissolution and anion-exchange resin. For each sample, around 3 mg of enamel powder was dissolved in 1 ml of hydrofluoric acid (2 M HF) overnight. Calcium fluoride (CaF_2) residue was separated by centrifugation and the solution was neutralized by adding 1 ml of potassium hydroxide (2 M KOH). Subsequently 1.5 ml of Amberlite™ anion-exchange resin was added to the solution to separate the PO_4^{3-} ions. After 24 h, excess solution was discarded, and the resin was eluted with 6 ml of ammonium nitrate (0.1 M NH_4NO_3). After 4 h, 0.1 ml of ammonium hydroxide (NH_4OH) and 3 ml of an ammoniacal solution of silver nitrate ($AgNO_3$) were added and the samples were placed in a thermostatic bath at 70 °C for 6 h, enabling the precipitation of Ag_3PO_4 crystals. Four standard samples of natural phosphorite (NBS120c) were included during the wet chemistry of each series of 10 samples to ensure that no isotopic fractionation occurred during the wet chemistry.

Oxygen isotope compositions were measured using a high-temperature elemental analyser (EA)-pyrolysis (Py) interfaced in continuous flow (CF) mode to an isotopic ratio mass spectrometer (IRMS) (EA-Py-CF-IRMS technique performed at UMR 5276 LGL; Fourel et al., 2011; Lécuyer et al., 2007). For each sample, five aliquots of 300 mg of Ag_3PO_4 were mixed with 300 mg of pure graphite powder loaded in silver foil capsules. Pyrolysis was performed at 1450 °C using a varioPYROcube™ elemental analyser interfaced with an Isoprime™. Measurements were calibrated with the standard samples of NBS120c phosphorite, whose value was fixed at 21.7‰ (V-SMOW; Lécuyer et al., 1993), and NBS127 barium sulphate with a value of 9.3‰ (V-SMOW; Hut, 1987). The average standard deviation for the Cova dels Xaragalls samples is 0.34 ± 0.04‰ (n ¼ 48) and 0.33 ± 0.07‰ (n ¼ 14) for the modern samples. Aliquots of silver phosphate were analysed several times a day in order to account for possible instrumental drift.

3.4. Oxygen isotope compositions of modern meteoric waters

Present-day $\delta^{18}O_{mw}$ values for the localities where the modern teeth samples were taken and for the Cova dels Xaragalls area (Vimbodí) were obtained using the Online Isotopes in Precipitation Calculator (OIPC; Bowen, 2017). This online software employs an algorithm based on datasets collected by the Global Network for Isotopes in Precipitation (GNIP), operated by the International Atomic Energy Agency and the World Meteorological Organization (IAEA/WMO, 2018) (Appendix A and C). Using the same approach as Fricke and O'Neil (1999) and Bernard et al. (2009), we calculated seasonal $\delta^{18}O_{mw}/T_{air}$ regressions using a sub-dataset of the IAEA-GNIP/ISOHIS dataset (2018) restricted to the Iberian Peninsula (Appendix B). This sub-dataset comprises monthly $\delta^{18}O_{mw}$ values obtained from 26 localities throughout the Iberian Peninsula ranging from 5 to 1380 m a.s.l. The current-temperature data for the Cova dels Xaragalls area are from Climate-Data.org (https://es.climate-data.org/) based on a climatic model using extended world climate data collected between 1982 and 2012 from the OpenStreetMap project.

3.5. Mutual ecogeographic range method and bioclimatic model

The mean annual temperatures (MAT) calculated from the $\delta^{18}O_p$ values of rodent teeth are compared with those derived from two alternative and independent palaeoenvironmental methods. The first, called the mutual ecogeographic range (MER) method, determines the present-day geographical region in which a given fossil species assemblage would be located through the intersection obtained from the overlap of the current distributions of each

Table 2
Oxygen isotope composition of tooth enamel phosphate ($\delta^{18}O_p$; ‰ V-SMOW) from rodent lower incisors from Cova dels Xaragalls. The table includes the stratigraphic layer, identified taxa and the conversion to the oxygen isotope composition of meteoric waters ($\delta^{18}O_{mw}$; ‰ V-SMOW) following the Royer et al. (2013a) oxygen isotope fractionation equation. SD, Standard Deviation.

Sample	Level	Taxa	Laterality	Location	$\delta^{18}O_p$	SD	$\delta^{18}O_{mw}$
CX45	C4	Apodemus cf. sylvaticus	right	isolated	16.6	0.2	−6.8
CX42	C4	Apodemus cf. sylvaticus	right	isolated	17.7	0.5	−5.8
CX44	C4	Apodemus cf. sylvaticus	left	isolated	17.9	0.2	−5.7
XG4B-5	C4	Apodemus sylvaticus	right	in situ	17.9	0.2	−5.7
CX46	C4	Microtus arvalis	right	in situ	18.2	0.5	−5.4
CX41	C4	Apodemus cf. sylvaticus	right	isolated	18.4	0.4	−5.3
XG4-2a	C4	Apodemus sylvaticus	left	in situ	18.5	0.5	−5.2
XG4-3a	C4	Apodemus sylvaticus	right	in situ	19.8	0.3	−4.1
XG4B-4	C4	Apodemus sylvaticus	left	in situ	20.8	0.3	−3.2
CX43	C4	Apodemus cf. sylvaticus	right	isolated	21.4	0.5	−2.8
XG4-1a	C4	Apodemus sylvaticus	left	in situ	22.2	0.1	−2.1
XG5-3	C5	Apodemus sylvaticus	left	in situ	16.3	0.3	−7.0
XG5-4	C5	Apodemus sylvaticus	right	in situ	17.4	0.3	−6.1
CX52	C5	Apodemus sylvaticus	left	in situ	17.5	0.3	−6.0
CX54	C5	Apodemus cf. sylvaticus	left	isolated	17.6	0.3	−5.9
CX53	C5	Apodemus cf. sylvaticus	left	isolated	19.0	0.9	−4.7
XG5-1	C5	Apodemus sylvaticus	left	in situ	19.6	0.3	−4.3
XG5-2	C5	Apodemus sylvaticus	left	in situ	19.7	0.4	−4.2
CX51	C5	Eliomys quercinus	right	in situ	19.8	0.3	−4.1
CX55	C5	Apodemus cf. sylvaticus	right	isolated	19.9	0.1	−4.0
XG5-5	C5	Apodemus sylvaticus	right	in situ	20.4	0.3	−3.6
XG6-4	C6	Apodemus sylvaticus	right	in situ	16.0	0.4	−7.3
XG6-3	C6	Apodemus sylvaticus	left	in situ	17.0	0.2	−6.4
XG6-2	C6	Apodemus sylvaticus	left	in situ	17.1	0.5	−6.3
XG6-1	C6	Apodemus sylvaticus	left	in situ	17.3	0.3	−6.2
CX64	C6	Apodemus sylvaticus	right	in situ	17.8	0.4	−5.8
CX65	C6	Apodemus cf. sylvaticus	left	in situ	19.3	0.4	−4.5
CX62	C6	Apodemus cf. sylvaticus	left	in situ	19.6	0.5	−4.3
CX63	C6	Apodemus cf. sylvaticus	left	in situ	19.6	0.2	−4.2
CX61	C6	Apodemus cf. sylvaticus	right	in situ	20.2	0.4	−3.8
XG6-5	C6	Apodemus sylvaticus	right	in situ	23.2	0.6	−1.3
XG7-3b	C7	Apodemus sylvaticus	left	in situ	14.6	0.2	−8.4
XG7-4a	C7	Apodemus sylvaticus	right	in situ	17.0	0.3	−6.4
CX71	C7	Apodemus sylvaticus	right	in situ	17.2	0.2	−6.2
XG7-1b	C7	Apodemus sylvaticus	right	in situ	17.4	0.8	−6.0
CX72	C7	Apodemus cf. sylvaticus	right	isolated	18.0	0.3	−5.6
CX73	C7	Apodemus cf. sylvaticus	left	isolated	18.3	0.2	−5.4
XG7-5a	C7	Apodemus sylvaticus	left	in situ	20.0	0.3	−3.9
XG7-2b	C7	Apodemus sylvaticus	right	in situ	20.3	0.4	−3.7
CX75	C7	Apodemus cf. sylvaticus	left	isolated	20.6	0.1	−3.4
CX74	C7	Apodemus cf. sylvaticus	left	isolated	21.5	0.4	−2.7
CX80	C8	Apodemus cf. sylvaticus	left	isolated	17.9	0.1	−5.6
CX81	C8	Apodemus cf. sylvaticus	right	isolated	18.2	0.3	−5.4
CX84	C8	Apodemus cf. sylvaticus	left	isolated	18.6	0.4	−5.1
CX83	C8	Apodemus cf. sylvaticus	left	isolated	18.7	0.4	−5.0
CX82	C8	Apodemus cf. sylvaticus	left	isolated	19.3	0.3	−4.5

species (Blain et al., 2009, 2016; López-García, 2011). The current climatic conditions of the intersecting area are used to infer the MAT. The MER estimations presented in this work have already been published by López-García et al. (2012). The second method, called the bioclimatic model (BM), is based on the adscription of small-mammal species to ten different climatic zones (Hernández Fernández, 2001; Hernández Fernández et al., 2007). This allows the calculation first of the Climatic Restriction Index (CRIi ¼ 1/n, where i is the climatic zone inhabited by the species and n is the number of climatic zones the species inhabit) and then the Bioclimatic Component (BCi¼(ΣCRIi)100/S, where S is the number of species). From the BC it is possible to calculate the MAT by means of a multiple linear regression developed specifically for the order Rodentia (Hernández Fernández, 2001; Hernández Fernández et al., 2007).

3.6. Statistical calculations

Ordinary least squares (OLS) regression was used to examine the relationship between the mean annual $\delta^{18}O_{mw}$ values and the mean March–June $\delta^{18}O_{mw}$ values from 26 Iberian localities. OLS was also used to examine the relationship between the mean annual $\delta^{18}O_{mw}$ values and the monthly mean air temperatures (Appendix B and C). The equations calculated by the OLS regression model were further used for calculations using transposed fits (Skrzypek et al., 2016). Uncertainties in temperature calculations were determined by applying error propagations according to the method developed by Pryor et al. (2014). Statistical analyses were performed with R v3.3.2 (R Core Team, 2017) and the Paleontological Statistics program - PAST3 (Hammer et al., 2001).

4. Results and discussion

The reconstruction of past air temperatures from the oxygen isotope composition of rodent teeth is a two-step procedure: 1) the measured $\delta^{18}O_p$ values of the fossil rodent teeth allow the estimation of the $\delta^{18}O$ values of local meteoric water ($\delta^{18}O_{mw}$) and, 2) the calculated $\delta^{18}O_{mw}$ values can be used to estimate past air

temperatures. Since pioneering works in the 1980's (Longinelli, 1984; Luz et al., 1984; Luz and Kolodny, 1985), many studies have explored the complex relationship between the oxygen isotope composition of vertebrate phosphatic tissues and body water, itself related to the oxygen isotope composition of ingested water, which ultimately derives from meteoric water. The oxygen isotope composition of body water is species-dependent, being controlled by both input and output oxygen fluxes as well as physiological factors such as basal metabolism and body temperature (Lindars et al., 2001; Longinelli, 1984; Luz et al., 1984; Podlesak et al., 2008). Over the last two decades, distinct species-dependent oxygen isotope fractionation equations relating $\delta^{18}O_p$ and $\delta^{18}O_{mw}$ have thus been experimentally determined (e.g. for rodents, D'Angela and Longinelli, 1990; Lindars et al., 2001; Luz and Kolodny, 1985; Navarro et al., 2004). Recently, using a large dataset that extends from 38° N to 65° N in Europe, Royer et al. (2013a) proposed a robust linear oxygen isotope fractionation equation for Muroidea teeth between $\delta^{18}O_p$ and $\delta^{18}O_{mw}$ values:

$$\delta^{18}O_p = 1.21\ (\pm 0.20) \times \delta^{18}O_{mw} + 24.76\ (\pm 2.70) \quad (1)$$

Equation (1) is used in this study to estimate the $\delta^{18}O_{mw}$ contemporaneous with MIS 3 in the Iberian Peninsula.

At mid and high-latitudes, mean annual $\delta^{18}O_{mw}$ values are linearly related to the regional mean annual air temperatures (Dansgaard, 1964; Rozanski et al., 1993). The $\delta^{18}O_{mw}$ values are mainly controlled by the water vapour source, the trajectories of humid air masses, seasonal variations of precipitation and the ambient air temperature during the process of condensation. During the warm season, $\delta^{18}O_{mw}$ values increase, whereas they decrease during the cold season. At a regional scale such as in Europe, a "continental effect" is observed, with decreasing $\delta^{18}O_{mw}$ values landward, and an "altitude effect", with $\delta^{18}O_{mw}$ values decreasing with increasing altitude, in response to the gradual removal of moisture from uplifted air masses with a preferential removal of the heavy isotope ^{18}O during condensation (e.g., Dansgaard, 1964). Several equations have been proposed for estimating past temperatures from $\delta^{18}O_{mw}$ at mid and high latitudes (e.g. Bernard et al., 2009; García-Alix, 2015; Lécuyer, 2014; Pryor et al., 2014; Rozanski et al., 1993; von Grafenstein et al., 1996). These equations are based on data related to different geographic scales, which can result in sizable differences in the estimations for air temperatures (Daux et al., 2005) when applied to specific regions such as the Iberian Peninsula.

4.1. Oxygen isotope composition of meteoric water in the Iberian Peninsula

Although numerous previous isotopic studies have attempted to characterize the climate of the Mediterranean Basin (Dansgaard, 1964; Gat et al., 2003; Gat and Carmi, 1970; Hartman et al., 2015; Lécuyer, 2014; Lécuyer et al., 2018), the Iberian Peninsula is not readily equated with any other Mediterranean region. Indeed, it is a complex territory in terms of climate due to its latitude range, its location between Atlantic and African-Mediterranean influences and its particularly complex orography, thus incorporating all the features of a small-scale continent (Font-Tullot, 2000). Indeed, Iberia plays a major role as a centre of secondary action in the mechanism of the general circulation of the atmosphere, as a consequence of air masses of different origin that converge in this region (Font-Tullot, 2000).

The current seasonal variation in the $\delta^{18}O_{mw}$ values interpolated for the Iberian Peninsula (OIPC data; Bowen, 2017; Appendix A; Fig. 3A) follows the isotopic pattern of mid and high latitudes (Dansgaard, 1964; Gat, 1980; Rozanski et al., 1993) with an increase in $\delta^{18}O_{mw}$ values in summer and a decrease in winter. Nonetheless, sizable differences between Iberia and higher-latitude localities, such as southwestern France, can be seen in the annual ranges of the $\delta^{18}O_{mw}$ values, with higher seasonal differences observed in Iberia (6.8–8.9‰) than in southern France (3.7–5‰). The differences between these two regions correspond to the presence of lower $\delta^{18}O_{mw}$ values in the Iberian Peninsula for the colder season in conjunction with notably higher $\delta^{18}O_{mw}$ for the warmer season. This phenomenon may be related to the motion of humid air masses that occurs in Iberia (Gat et al., 2003). During summer, most of the Iberian Peninsula (with the exception of the Cantabrian to Atlantic seaboards) is under the influence of continental tropical air mass from North Africa, which impose hot and arid summers (Font-Tullot, 2000). Before reaching Iberia, the continental tropical air mass from North Africa becomes enriched by the heavy isotope ^{18}O during its transport over the Mediterranean Sea. Likewise, the complex Iberian orography characterized by high and mountainous relief causes large seasonal climatic amplitudes, which may influence large annual ranges of $\delta^{18}O_{mw}$.

Considering the described climatic singularities of the Iberian Peninsula, a specific linear regression is therefore established between the mean annual $\delta^{18}O_{mw}$ values and the mean annual air temperatures. The linear regression of the GNIP data provides the following equation (Fig. 4A; Appendix B):

$$MAT\ (^{o}C) = 2.38(\pm 0.10) \times \delta^{18}O_{mw} + 28.19(\pm 0.58)\ \text{with}\ R^2 = 0.65\ (n = 304;\ p < 0.0001;\ S_{y/x} = 3.6) \quad (2)$$

4.2. Oxygen isotope composition of present-day rodents from the Iberian Peninsula

4.2.1. $\delta^{18}O_p$ intra-pellet variability

A key factor in understanding the isotopic variability recorded in rodent teeth is the formation of rodent accumulations, leading to questions of how and when these accumulations were produced (e.g. Royer et al., 2013a, b). In cases where rodent fossil accumulations are produced by predators, sampling bias may result from defined hunting territories, which vary among predators as a function of ecology and the local orography. The $\delta^{18}O_p$ values measured in fourteen modern rodents collected in northeastern Iberia range from 16.1‰ to 20.2‰ (Table 1; Appendix A). Despite the limited number of specimens, the variations in the $\delta^{18}O_p$ values between different incisors within each pellet are relatively low, with differences between the minimum and maximum $\delta^{18}O_p$ values ranging from 0.5 to 1.9‰. The intra-pellet variation of $\delta^{18}O_p$ is lower than 1‰ in the case of Serinyà (0.7‰), El Catllar (0.5‰) and Moià (0.9‰). In the case of Moià, it should be noted that an extra specimen collected outside of the pellet shows a distinct value lower by 2‰. The higher variability in the pellets from Prades (1.9‰) and Balaguer (1.5‰) could be related to the complex orography in the surrounding region, as a result of which the activity of the predator may cover a large altitude range (from 200 to 1000 m a.s.l.) within a rather restricted area. The predator thus has access to prey that are more isotopically variable due to the altitude effect. From the intra-pellet ranges observed in this work, we calculated an average range of 1.1 ± 0.5‰ (SD = 0.5‰). The isotopic ranges in the current study are bracketed by the minimum (0.2‰) and the maximum (5.2%) values measured by Royer et al. (2013a) on pellets, with a mean value of 2.9 ± 1.1‰ (SD = 1.6‰). Nevertheless, this work small number of samples could hide more significant variations. Barham et al. (2017) observed greater intra-specific variability (up to 2‰) for $\delta^{18}O_p$ values among individuals from equal laboratory conditions, warning of greater variation in natural

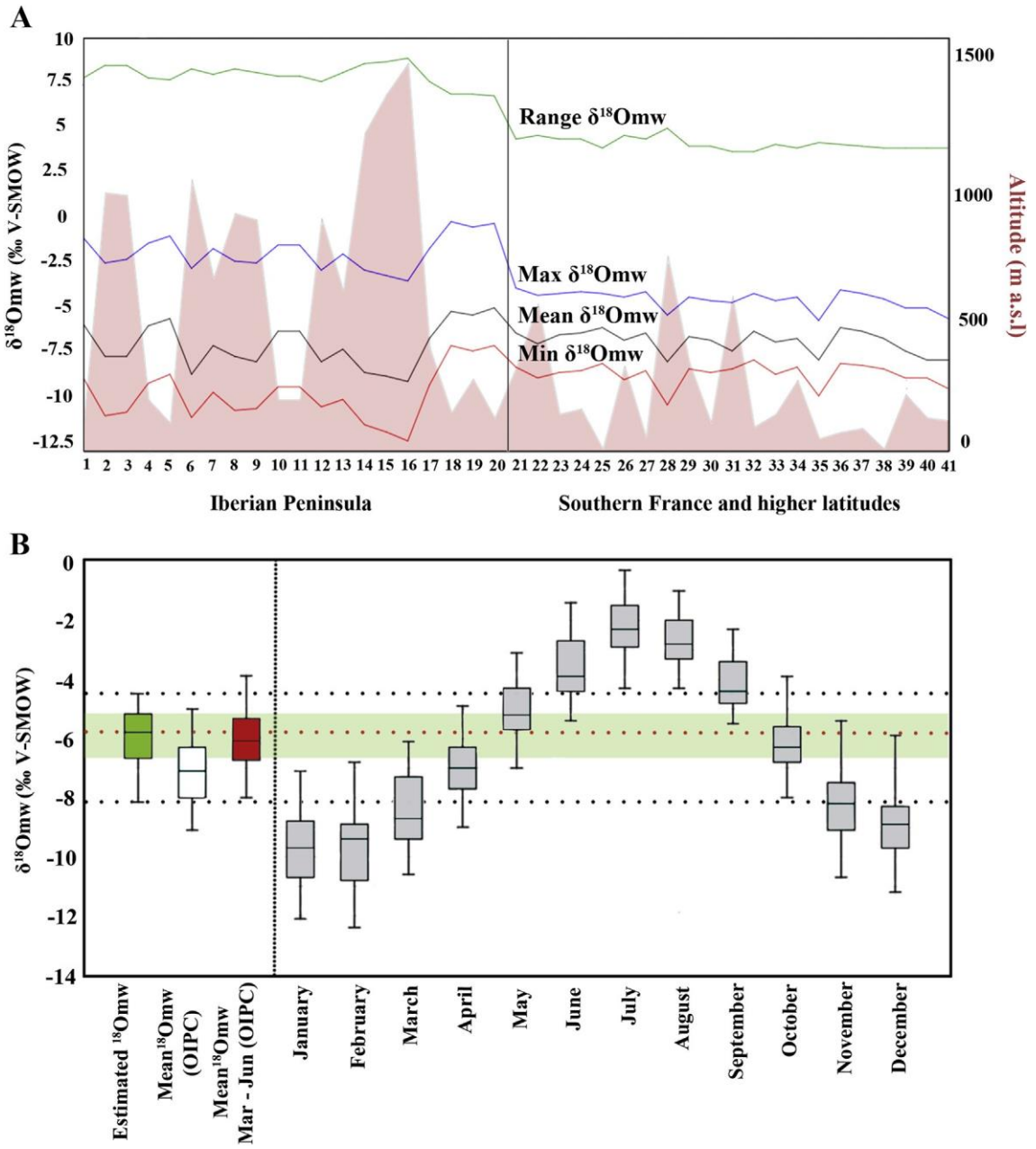

Fig. 3. A) Oxygen isotope composition (‰ V-SMOW) of meteoric waters ($d^{18}O_{mw}$) from localities in the Iberian Peninsula, southern France and other localities from higher latitudes (numbers 1 to 20 and 21 to 41, respectively; detailed information available in Appendix A), using data from OIPC software (Bowen, 2017). The red, black, blue and green curves represent the minimum, the maximum, the mean annual and the range of $d^{18}O_{mw}$ values respectively for each locality. The altitude is indicated in light red (m above sea level) for each locality. B) Box plot representation of $d^{18}O_{mw}$ estimated from the oxygen isotope composition of phosphate from present-day Iberian rodent teeth (green box plot); mean annual values (white box plot), mean values from March to June (red box plot) and monthly means (grey box plots) obtained from OIPC software (Bowen, 2017). The black dashed lines indicate the limits of the estimated values, and the red line their mean; the green fringe shows the estimated values between the 1st and 3rd quartile. (For interpretation of the references to color in this figure legend, the reader is referred to the Web version of this article.)

conditions.

4.2.2. Time interval recorded by rodent lower incisors

Various factors lead rodent tooth phosphate to record a $d^{18}O_{mw}$ value that corresponds to a short time interval of less than a season (Royer et al., 2013a). Small-sized animals, such as the great majority of present-day rodents, have a rapid water turnover (according to Podlesak et al. (2008) woodrats reach isotopic equilibrium two weeks after a change of drinking water), and their teeth are mineralized rapidly, a few days after their birth (Blumenthal et al., 2014; Hillson, 2005). Furthermore, rodent incisors are characterized by their continuous growth throughout the life of the individual, offering opportunities to provide a record of the last days before the individual's death. The growth time of the incisor is species-dependent, mainly in relation to their size and body weight. The renewal time for the lower incisors is generally around 30e60 days (Coady et al., 1967; Klevezal, 2010; Klevezal et al., 1990), whereas the murine species of the genus Apodemus tend more towards 50e60 days (Klevezal, 2010). In the case of the murids, on the basis of the dentin thickness increments, Klevezal (2010) noted that the daily growth rate of the incisor may also vary according to the diet and especially according to the season

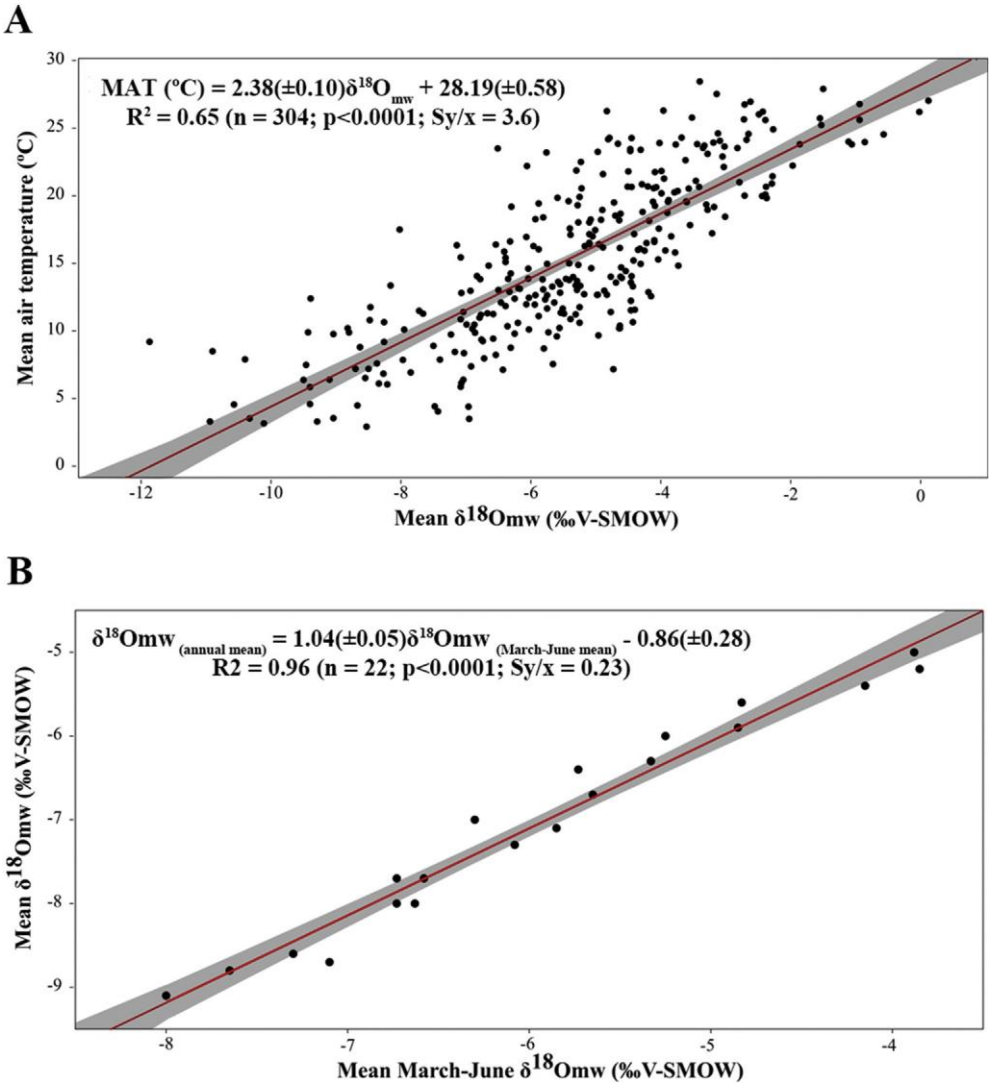

Fig. 4. Proposed corrections for palaeotemperature reconstruction in northeastern Iberia. A) Linear regression model (OLS equation) relating monthly mean $d^{18}O_{mw}$ values and monthly mean air temperatures, from available dataset for Iberia from the Global Network of Isotopes in Precipitation, operated by the International Atomic Energy Agency and the World Meteorological Organization (IAEA/WMO, 2018); B) Linear regression model (OLS equation) between current mean annual $d^{18}O_{mw}$ and mean MarcheJune $d^{18}O_{mw}$ values from Iberian localities included in this study, using data from OIPC software (Bowen, 2017). Uncertainty with 95% confidence interval indicated in light grey. Further information in Appendix B and Appendix C.

and the age of the specimen. The gestation period of the wood mouse extends over 20e30 days, and weaning takes place between 13 and 21 days after birth, when the development of the incisors starts (Sånchez-Gonzålez et al., 2016; Palomo et al., 2007). Thus, the $d^{18}O_p$ recovered from a murid lower incisor contains integrated oxygen isotope information from the last two months of the individual's life and avoids any weaning effect as recorded in rooted adult molars (Gehler et al., 2012, 2011; Jeffrey et al., 2015; Royer et al., 2013a). Indeed, pellets from Moiï, Prades and Serinyï were recovered between the end of August and the beginning of September. The $d^{18}O_{mw}$ values estimated from the $d^{18}O_p$ values of the rodent incisors recovered from these pellets match those documented by the IAEA/WMO stations for the AprileMay (Serinyï) and MayeJune (Moiï and Prades) periods.

4.2.3. Preferential time interval of rodent accumulation reflected by $d^{18}O$

The mean $d^{18}O_p$ value calculated for the fourteen new present-day samples is 18.7 ± 0.5‰, which is higher than most values recorded at higher latitudes (Fig. 1A; Appendix A). By combining these fourteen $d^{18}O_p$ values with fifteen previously published by Royer et al. (2013a) from Iberian locations (Fig. 1A), we obtained a set of $d^{18}O_p$ values ranging from 13.1‰ to 22.2‰, with a mean value of 17.7 ± 0.6‰ (SD ¼ 1.9‰). When these $d^{18}O_p$ values are converted into $d^{18}O_{mw}$ values using equation (1) and then compared to current $d^{18}O_{mw}$ data (OIPC data; Bowen, 2017), they are seen mainly to match the spring and the beginning of summer (between March and June) or the autumn (between September and November), this pattern is not as clear in higher latitudes such as southwestern France (Appendix A; Fig. 3B). The mean $d^{18}O_{mw}$ values estimated from present-day Iberian samples are closer to the mean value corresponding to the MarcheJune time span, being slightly higher (by þ 1.1‰) than the expected mean $d^{18}O_{mw}$ values (IAEA/WMO) corresponding to the MarcheMay interval in each location. This slight overestimation of $d^{18}O_{mw}$ values translates into overestimated annual air temperatures (by þ 2.6‰). As previously noted, the Iberian Peninsula is characterized by a large seasonal amplitude of $d^{18}O_{mw}$ values, and the MarcheJune period is one of

the most variable in $\delta^{18}O_{mw}$ values (Fig. 3A). Indeed, the variation is around 5‰ between March and June, whereas it only reaches 2–3‰ at higher latitudes such as southwestern France.

Predator-prey interactions can influence oxygen isotope temporal information record. Generally, rodents show increased population sizes and greater outdoor activity from spring to autumn, whereas their activity is reduced in winter (Le Louarn and Quéré, 2003). For northern latitudes and higher altitudes, the reproductive activity of the wood mouse mainly occurs between spring and summer and ceases during winter. In contrast, in Mediterranean areas such as northeastern and southern Spain, or in areas with a Mediterranean influence (such as Portugal), the pattern of reproductive activity is reversed, starting in autumn and ending in spring, with summer always being the rest period (Fons and Saint Girons, 1993; Moreno and Kufner, 1988; Rosário and Mathias, 2004; Sans-Coma and Gosalbez, 1976; Sunyer et al., 2016). The great variability in the reproductive cycles of the wood mouse is related to its great capacity to adapt to the availability of food and, which is partially influences by local climatic and environmental conditions (Fons and Saint Girons, 1993). In the Mediterranean Basin, high temperatures coupled with low summer rainfall, sometimes generating drought periods, may explain the absence of reproduction in summer and the occurrence of population peaks in spring (Moreno and Kufner, 1988; Rosário and Mathias, 2004). Summer is considered a period of stress for this species living in Mediterranean environments, as also expressed by a low survival rate (Rosário and Mathias, 2004).

In parallel, the observed oxygen isotopic variations in rodent teeth can be partly explained by the season of prey capture (Royer et al., 2013a, 2013b). At mid to high latitudes, the dynamic and structure of raptor populations (breeding, density, natality and migration) are affected by rodent abundances in spring-summer (Norrdahl and Korpima, 2002; Salamolard et al., 2000). The success of the predator population depends to a large extent on the abundance of its prey during the breeding season. This phase is the optimal period for predator hunting activity. For instance, Sundell et al. (2004) have shown that the success of avian predators at high latitudes (60° N) is strongly correlated with the abundance of rodents, showing a seasonal numerical response. In addition, birds of prey tend to improve their hunting efficiency during the breeding season, to meet the energy requirements for feeding their young. In the Iberian Peninsula, the most common rodent predators, owls (Tyto alba, Athene noctua, Otus scops, Asio otus, Bubo bubo, Asio flammeus, Strix aluco), usually have their reproduction and breeding period between spring and the beginning of summer (Manzanares, 2012) (Appendix D). Consequently, the probability of rodent capture by owls is highest during this period.

It is therefore considered that rodent $\delta^{18}O_p$ values mainly reflect the $\delta^{18}O_{mw}$ values of the March–June period in Iberian Peninsula localities (Fig. 3B). We propose a linear regression based on OIPC data (Bowen, 2017) between the $\delta^{18}O_{mw}$ values of the March–June period and the mean annual $\delta^{18}O_{mw}$ values. This can be applied to Iberian rodent populations to calculate the mean annual $\delta^{18}O_{mw}$ values in the fossil record (Fig. 4B):

$$\delta^{18}O_{mw\ (annual\ mean)} = 1.04(\pm0.05) \times \delta^{18}O_{mw\ (March\text{-}June\ mean)} - 0.86(\pm0.28) \text{ with } R^2 = 0.96 \ (n = 22;\ p < 0.0001;\ S_{y/x} = 0.23) \quad (3)$$

4.3. Oxygen isotope compositions from fossil rodent teeth: from $\delta^{18}O_p$ values to temperatures in the Iberian Peninsula

In the Iberian Peninsula, the period of maximal rodent density and predator activity corresponds to the spring-early summer months. We suggest that a similar interpretation could be applied to rodent fossil assemblages sampled from Late Pleistocene deposits from Iberia. Variability of $\delta^{18}O_p$ values obtained should be explored from multiple teeth within each stratigraphic level as an indicator of intra-level distribution to evaluate inter-annual climate instability. This variability can be minimal (<4‰) or very substantial (>8‰). In the case of positive asymmetry in the frequency distribution of $\delta^{18}O_p$ values, a bias due to a warm and arid period can be surmised, whereas a negative asymmetrical distribution of values could be related to individual captures during the winter period (Royer et al., 2013b, 2014). Furthermore, to calculate an average value, we recommend using median $\delta^{18}O$ values, which are less subject to extreme values. If exploring this variability could help to understand the isotopic signal, it is nonetheless based on the working hypothesis of a main accumulation during one season. The confidence in these interpretations should always be cautiously taken that could also result from a seasonal effect alone. Complexity is also added by the structure of fossil deposits, where the isotopic composition of rodent teeth could reflect either a unique short event or long periods of accumulation (from a couple of years to thousands of years) yet distinguishing these two possibilities is extremely challenging.

Estimations of palaeotemperatures usually require a two-step procedure involving two linear equations: 1) from $\delta^{18}O_p$ to $\delta^{18}O_{mw}$; 2) from $\delta^{18}O_{mw}$ to air temperatures. Considering the possible seasonality of the rodent assemblages and the regional peculiarities of the Iberian Peninsula, the following three-step strategy is proposed for the reconstruction of estimated palaeotemperatures from rodent tooth $\delta^{18}O_p$ accumulated in the Iberian Peninsula:

1) Estimation of $\delta^{18}O_{mw}$ from $\delta^{18}O_p$, employing the linear oxygen isotope fractionation equation determined by Royer et al. (2013a) (1), using the median $\delta^{18}O_p$ value from a given level.
2) When the rodent isotopic record is preferentially biased towards air temperatures of the spring-summer months, we also recommend an additional equation (3) that can be applied to $\delta^{18}O_{mw}$ for the March–June period in order to obtain the corresponding mean annual $\delta^{18}O_{mw}$ (3).
3) Estimation of air temperatures from $\delta^{18}O_{mw}$, using the linear regression model specific to Iberia developed in this work, relating the mean annual $\delta^{18}O_{mw}$ and the mean annual air temperatures (2).

Nonetheless, one additional correction should be performed before $\delta^{18}O_{mw}$ values can be quantitatively estimated, related to the ice volume effect. During glacial periods, the oxygen isotope composition of seawater changes in response to the fluctuations in the volume of continental ice. Any change in the seawater oxygen composition is passed on to the surface hydrological cycle at a globe scale, which includes the oxygen isotope composition of meteoric waters. For instance, the global seawater $\delta^{18}O$ value increased by 1.0 ± 0.1‰ during the Last Glacial Maximum, whereas during MIS 3 the sea level was around 50 m below the present-day sea level. This sea level fluctuation may have contributed to an increase in the global $\delta^{18}O_{mw}$ value by +0.6‰, resulting in a bias in calculated air temperatures of +1 °C (see Schrag et al., 2002).

4.4. Palaeoenvironmental and palaeoclimatic reconstruction of Cova dels Xaragalls

The oxygen isotope composition of rodent incisor enamel from different layers within Cova dels Xaragalls ranges from 14.6‰ to 23.2‰, with a total variation of 8.6‰ (Fig. 5; Table 3). Mean $\delta^{18}O_p$ values for each specific horizon sampled are fairly constant over the

sequence, varying between 18.4‰ (layer C7) and 19.0‰ (layer C4). The median $\delta^{18}O_p$ values vary only slightly from 18.2‰ (layer C7) to 19.3‰ (layer C5), but remain largely similar to the means, with the mean $\delta^{18}O_p$ never exceeding more than 0.6‰ above the median $\delta^{18}O_p$ value. The oxygen isotope compositions of M. arvalis (18.2‰; layer C4) and E. quercinus (19.8‰; layer C5) keep within the general range obtained from A. sylvaticus measurements and have no influence either on the mean or median values. All sedimentary layers show a normal distribution of data (Shapiro-Wilk test, p-value>0.01). Sizeable intra-level variations are observed (1.4‰e 7.2‰). Layers C8 and C5 are characterized by the lowest intra-level variability in $\delta^{18}O_p$ values (1.4‰ and 4.1‰, respectively), lower standard deviations (0.5‰ and 1.4‰, respectively) and the highest medians (18.6‰ and 19.3‰, respectively). By contrast, layers C7, C6 and C4 show higher $\delta^{18}O_p$ variability (6.9‰, 7.2‰ and 5.6‰, respectively), higher standard deviations (2.1‰, 2.1‰ and 1.8‰, respectively) and lower medians (18.2‰, 18.5‰ and 18.4‰, respectively).

The low to moderate $\delta^{18}O_{mw}$ intra-level ranges recorded in the Cova dels Xaragalls fossil deposits, which vary from 1.1 to 5.9‰ (Table 3), are lower than the current seasonal amplitude for $\delta^{18}O_{mw}$ values at Vimbodí-Poblet (8.5‰; OIPC data) and the average seasonal amplitude of $\delta^{18}O_{mw}$ values for Iberia (8‰; OIPC data; Fig. 3a). These patterns suggest that small-mammal remains preferentially accumulated seasonally, which would have probably been during the spring-early summer months. Taphonomic analyses suggest that the predator responsible for the rodent accumulation throughout the Cova dels Xaragalls sequence is Athene noctua (López-García et al., 2012). This nocturnal bird of prey feeds mainly on insects, but also on small mammals, frogs and birds. It is a sedentary species that inhabits restricted territories (around 0.8 km^2), and within the Iberian Peninsula it breeds from April to May in tree holes or rock fissures (Andrews, 1990; Manzanares, 2012; Mikkola, 1983; IUCN, 2018). At higher altitudes, this species is known to hunt small mammals preferentially during winter (Andrews, 1990; Delibes et al., 1983). Contrary, in Mediterranean areas some studies have quantified high rates of small-mammal consumption during both spring and autumn (e.g. Sekour et al., 2011). Furthermore, despite the low $\delta^{18}O$ variability observed, this owl tends to produce important digestion damage on teeth (Andrews, 1990), so an unknown influence in the oxygen isotopic signal produced by the digestive enzymes can never be discarded. Considering Barham et al. (2017), digestion inflicted by Tyto alba supposed ~0.7‰ decreases from the original $\delta^{18}O_p$ values.

The high variation in $\delta^{18}O_p$ values observed within the layers could be related to seasonal or climatic fluctuations. Combining median data with ranges and standard deviations and taking into account previous environmental data inferred from the small-vertebrate and charcoal studies of the site (López-García et al., 2012; Vallverdú et al., 2012), let us to consider that layers C6, C7 and C4 show a degree of climatic variation in comparison to layers C8 and C5, which seem relatively more stable (Table 3; Fig. 5). Layers C6 and C4 show very high $\delta^{18}O_p$ values (>22‰), which could be related to water ^{18}O enrichment due to specially warm summer or arid events (Jeffrey et al., 2015; Royer et al., 2013b). By contrast, low $\delta^{18}O_p$ values such as those from layer C7 (<15‰) could be related to the predation of specimens in the cold season or in an exceptionally cold spring. The different altitudes at which the predator may have been hunting or even different sources of water ingested by hunted rodents (e.g. stagnant waters or snow melting) may also explain a part of these variations (Barham et al., 2017; Peneycad et al., 2019; Royer et al., 2013b). Indeed, Cova dels Xaragalls is surrounded by a mountainous environment with highly variable altitudes at a kilometre scale. López-García et al. (2012) indicate an inverse relationship between the temperatures and the amount of precipitation, with the warmest layers being the driest (C5 and C8) and the coldest layers being the wettest (C3-C4 and C6). These pluviometric changes could have magnified the variability in the oxygen isotope composition of layers C4 and C6. However, the global picture of slight inter-level variation, both for means and medians, indicates rather stable climatic conditions throughout the sequence, an interpretation that supports results from previous studies based on small-mammal assemblages and charcoal.

For each sedimentary level, mean annual temperatures (MAT) were calculated based on median $\delta^{18}O_p$ values and following the protocol previously proposed in section 4.4 using equations (1)e(3). The estimated MATs vary between 11.2 ± 2.6 °C and 13.6 ± 2.7 °C (Table 3; Fig. 6). These temperatures are slightly lower than the current MAT recorded at Vimbodí-Poblet (13.6 °C; Climate-Data.org), with the difference ranging from −2.4 °C (C7) to −1.5 °C (C8), except for layer C5, which recorded air temperatures comparable to present-day temperatures. The MAT temporal trend calculated from the $\delta^{18}O_p$ record is reasonably similar to that obtained by the mutual ecogeographic range (MER; López-García et al., 2012) and bioclimatic model (BM) reconstruction methods (Fig. 6). However, an offset of a few degrees is observed between the three methods, remaining small enough to fall within the confidence intervals of the techniques employed.

Previous anthracological studies performed at Cova dels Xaragalls have revealed low taxa diversity, which is related to the predominance of Pinus-type sylvestris throughout the sequence (more than 75%). This is a common feature of Late Pleistocene vegetation formations in northeastern Iberia due to the harsher climatic conditions, suggesting that Cova dels Xaragalls had a cooler climate than at present and a landscape dominated by open forests (López-García et al., 2012). Nevertheless, relative abundances up to 50% of the wood mouse, which is mainly associated with forests or forest margins, are uncommon during cold climate stages because species more associated with open landscapes are usually found. The location of Cova dels Xaragalls within Poblet Forest may have provided a suitable environment for species with generalist requirements, protected by low-altitude woodland formations and buffered climatic conditions. Recent morphological and morphometric studies performed on M. agrestis and M. arvalis remains sampled from levels C4-C6 have pointed to a possible increase in humidity levels, which in a Mediterranean context can be related to an extension of forest cover (Luzi, 2018). A correlation between layer C5 and interstadial phase IS13 or 14 (ca. 50e55 ka) was tentatively suggested by López-García et al. (2012), despite the fact that the biodiversity recorded in this level was not reliable due to the low abundance of individuals. Nonetheless, oxygen isotope ratios of rodent teeth from layer C5 are relatively enriched in ^{18}O with a small standard deviation, reflecting a MAT comparable to the present (13.6 °C). This observation thus confirms the temporal trends inferred from the MER and BM models. It also agrees with the documented faunal biodiversity in the interstadial context that prevailed during the deposition of layer C5. Even though the climatic conditions recorded throughout the sedimentary sequence seem to be slightly cooler than nowadays, our study raises the possibility that warm air temperatures close to Holocene conditions could have occurred during MIS 3 in the northeast of Iberia.

5. Conclusions

Oxygen isotope compositions were measured in rodent teeth accumulated in modern owl pellets from five different sites located in northeastern Iberia and complemented with previously published $\delta^{18}O$ results from rodent teeth from the Iberian Peninsula. The peculiar orography and climatic mode of the Iberian Peninsula

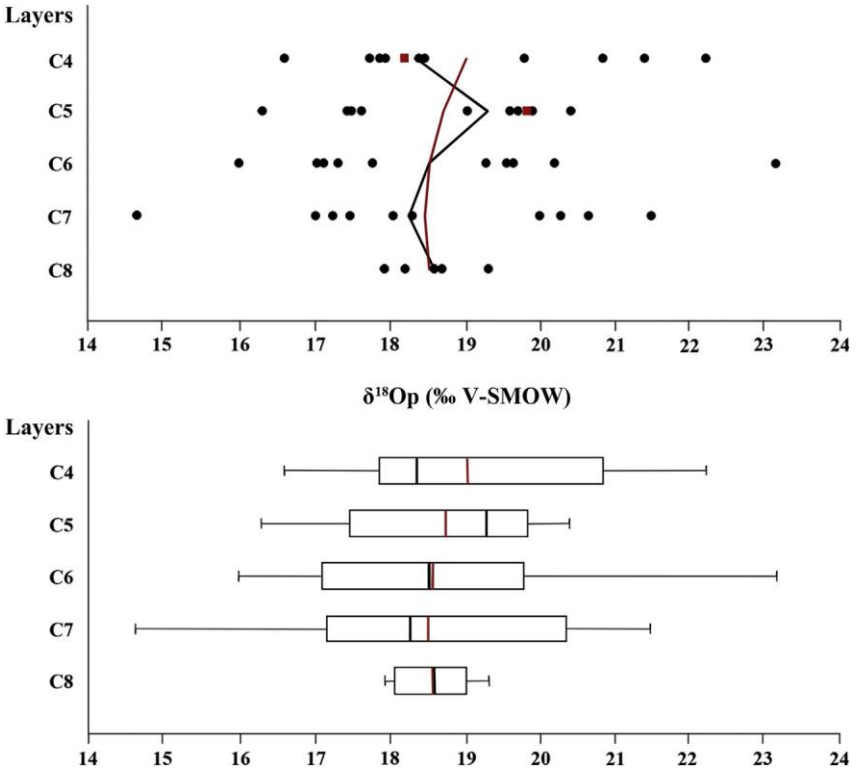

Fig. 5. Oxygen isotope composition of rodent incisor enamel ($d^{18}O_p$; ‰ V-SMOW) from the Cova dels Xaragalls samples. Above, distribution of $d^{18}O_p$ values per layer, with mean (red) and median (black) curves. Red squares illustrate the Microtus arvalis (C4) and Eliomys quercinus (C5) samples; black points identify the Apodemus sylvaticus samples. Below, box plots of the $d^{18}O_p$ values per layer, with mean (red) and median (black) indicated; the bars cover the full range of the values; the boxes extend from the 1st to 3rd quartile. (For interpretation of the references to color in this figure legend, the reader is referred to the Web version of this article.)

Table 3
Minimum, maximum, mean, median, standard deviation and range of oxygen isotope composition of incisor enamel phosphate ($d^{18}O_p$; ‰ V-SMOW) from fossil rodents recovered from Cova dels Xaragalls; conversion to the oxygen isotope composition of meteoric waters ($d^{18}O_{mw}$; ‰ V-SMOW); and, mean annual temperature estimations (MAT; ° C), including seasonality and sea-level corrections of $d^{18}O_{mw}$.

	Levels	C4	C5	C6	C7	C8
	n	11	10	10	10	5
$d^{18}O_p$	Min	16.6	16.3	16.0	14.6	17.9
	Max	22.2	20.4	23.2	21.5	19.3
	Mean	19.0	18.7	18.6	18.4	18.5
	Median	18.4	19.3	18.5	18.2	18.6
	Range	5.6	4.1	7.2	6.9	1.4
	SD	1.8	1.4	2.1	2.1	0.5
$d^{18}O_{mw}$	Min	−6.8	−7.0	−7.3	−8.4	−5.6
	Max	−2.1	−3.6	−1.3	−2.7	−4.5
	Mean	−4.8	−5.0	−5.1	−5.3	−5.1
	Median	−5.3	−4.5	−5.2	−5.5	−5.1
	Range	4.7	3.4	5.9	5.7	1.1
MAT	$d^{18}O_{mw}$ - seasonality correction	−6.3	−5.6	−6.2	−6.5	−6.2
	$d^{18}O_{mw}$ - sea level correction	−6.9	−6.2	−6.8	−7.1	−6.8
	MAT (^{0}C)	11.7	13.6	12.0	11.2	12.1
	SD	1.3	1.4	1.3	1.3	1.8
	Error margin	2.5	2.7	2.6	2.6	3.5

are emphasized by this study, which documents low $d^{18}O_p$ values and a large annual range of $d^{18}O_{mw}$ in comparison to southern France. On the basis of recent $d^{18}O_{mw}$ values extracted from IAEA/WMO databases, the oxygen isotope composition of contemporaneous Iberian rodent tooth samples reflects spring and early summer $d^{18}O_{mw}$ values. Consequently, the estimated mean $d^{18}O_{mw}$ values are closer to the March–June mean $d^{18}O_{mw}$ value than to the expected March–May mean $d^{18}O_{mw}$ value. The most likely cause is a preferential accumulation of rodent remains during this period, associated with enhanced predation activity. This interpretation is supported by ethological studies that suggest a higher probability of prey capture by owls from Iberia during the spring-early summer months as a consequence of the rising number of murid specimens. The oxygen isotope compositions recorded in present-day rodent tooth samples correspond to $d^{18}O_{mw}$ values contemporaneous with the two months prior to the deposition of the pellets by the predator. This is consistent with histological studies of genus Apodemus, which completes the renewal of its lower incisors in about two months.

In fossil assemblages, where the phenomenon of the palimpsest is common, observed $d^{18}O$ variations in rodent tooth enamel samples can be related both to intra-annual and to inter-annual changes in air temperature. Whenever possible, it is necessary to ascertain whether $d^{18}O_p$ intra-level variations are more related to the seasonality of samples or to climatic fluctuations. In addition, for Iberian palaeoenvironmental reconstructions based on $d^{18}O_p$, singular $d^{18}O_{mw}$ seasonal amplitudes and the preferential formation of rodent accumulations in the warm season could lead to an overestimation of the annual $d^{18}O_{mw}$ values and consequently of the mean annual air temperatures. This work has proposed two solutions for calculating mean annual temperatures: the development of a specific $d^{18}O_{mw}/T_{air}$ regression equation designed for the Iberian environmental context (2) and a regression equation that relates the March–June $d^{18}O_{mw}$ to the mean annual $d^{18}O_{mw}$ in order to correct the seasonal bias recorded in rodent tooth apatite resulting from the probable preferential accumulation of rodent remains in the warm season (3).

Finally, rodent incisor enamel sampled from layers C8 to C4 in

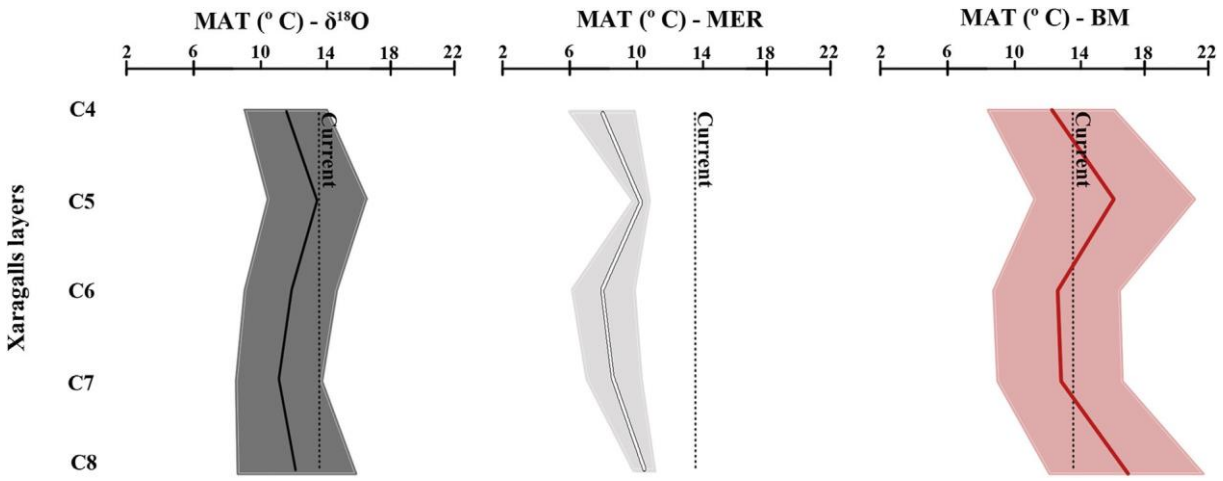

Fig. 6. Mean annual temperature (MAT; °C) reconstructed for the Cova dels Xaragalls layers using the oxygen isotope composition ($\delta^{18}O$) of rodent incisor enamel, the mutual ecogeographic range (MER) method and the bioclimatic model (BM). Dashed lines correspond to the current MAT at Vimbodí, and the shaded fringes to the error associated with each method.

Cova dels Xaragalls is characterized by low to moderate $\delta^{18}O_p$ intra-level variations never surpassing present-day annual $\delta^{18}O_{mw}$ variability. The parsimonious hypothesis is that the small-mammal remains were preferentially accumulated during equivalent seasons, most likely during spring-early summer months. The inter-level variations observed in C7, C6 and C4 could be related to high seasonal amplitude or high-frequency climatic fluctuations. However, the $\delta^{18}O_p$ variations suggest rather steady-state climatic conditions throughout the sequence with mean annual temperatures lower than current ones (−2.4 °C to −1.5 °C), except for layer C5, which records similar mean annual temperatures to those at present (13.6 ± 2.7 °C). This observation supports the correlation between layer C5 and interstadial phase IS13 or 14 (ca. 50e55 ka). Comparison with different models of palaeotemperature reconstruction for the deposit at Cova dels Xaragalls demonstrates homogeneity in the climatic signal.

Acknowledgements

The authors are grateful to Aitor Burguet Coca, Joan Burguet Ardiaca, Marta Puig Domènech, David Funosas, Marius Domingo de Pedro and Josep Maria Vergès for providing pellet samples. We also thank the team from the Laboratoire de Géologie of Lyon for allowing us to perform the isotope analysis, especially to Romain Amiot and Magali Seris. We also thank Christiane Denys, Emmanuelle Stoetzel and Hugues-Alexandre Blain for their help and advice during the preparation of the manuscript. We are also grateful to two anonymous reviewers for their comments which helped in improving the scientific content of this study. M. Fernández-García was beneficiary of a PhD scholarship during this manuscript writing funded under the Erasmus Mundus Programme e International Doctorate in Quaternary and Prehistory. J.M. López-García was supported by a Ramón y Cajal contract (RYC-2016-19386), and the research work of A. Rodríguez-Hidalgo was financed by the Subprograma Juan de la Cierva (FJCI-2015-24144), both with financial sponsorship from the Spanish Ministry of Science, Innovation and Universities.

Appendix A

Detailed data from localities in the Iberian Peninsula, southern France and other higher-latitude localities, with oxygen isotope compositions of tooth enamel phosphate from modern rodent teeth (this work and Royer et al., 2013a). Included for each locality is altitude (m a.s.l.); number of $\delta^{18}O$ samples (n); mean $\delta^{18}O$ from phosphates ($\delta^{18}O_p$; ‰ V-SMOW); mean and median estimated $\delta^{18}O$ from meteoric waters ($\delta^{18}O_{mw}$; ‰ V-SMOW) (following the Royer et al. (2013a) oxygen isotope fractionation equation); mean, ranges and monthly values of $\delta^{18}O_{mw}$ (OIPC data; Bowen, 2017). In dark grey, location of estimated mean $\delta^{18}O_{mw}$ from present-day samples within present-day $\delta^{18}O_{mw}$ values throughout the year; in light grey, location of all $\delta^{18}O_{mw}$ estimated in a given locality; red square, time of pellet recovery.

Appendix B

Available dataset of Iberian sites from the Global Network of Isotopes in Precipitation created by the International Atomic Energy Agency and the World Meteorological Organization (IAEA/WMO, 2018), employed to develop the linear regression model (OLS equation) relating the monthly mean $\delta^{18}O_{mw}$ and monthly mean air temperatures (Fig. 5A). Included for each site/month is latitude, longitude, altitude (m a.s.l.), number of samples (n), mean oxygen isotope composition of meteoric waters ($\delta^{18}O_{mw}$; ‰ V-SMOW) and mean air temperatures (°C).

Appendix C

Current oxygen isotope compositions of meteoric waters ($\delta^{18}O_{mw}$; ‰ V-SMOW) from Iberian localities and Corsican localities: mean from March to June and annual mean. Data are provided by the Online Isotopes in Precipitation Calculator, derived from the International Atomic Energy Agency/World Meteorological Organization Global Network for Isotopes in Precipitation (Bowen, 2017). These data are used to develop the linear regression model (OLS equation) between current mean annual $\delta^{18}O_{mw}$ and mean MarcheJune $\delta^{18}O_{mw}$ values (Fig. 5B).

Appendix D

Ecological data for the most common owls from the Iberian Peninsula: breeding season, reproduction and migration behaviour. Based on Manzanares (2012).

Appendix E. Supplementary data

Supplementary data to this article can be found online at https://doi.org/10.1016/j.quascirev.2019.04.035.

References

Andrews, P., 1990. Owls, Caves and Fossils. Predation, Preservation and Accumulation of Small Mammal Bones in Caves, with an Analysis of the Pleistocene Cave Faunas from Westbury-sub-Mendip, Somerset, UK. The University of Chicago, Chicago.

Arrizabalaga, Á., 2004. Paleoclimatología y cronología del Würm reciente: un intento de síntesis. Zephyrus 57, 27e53.

Barham, M., Blyth, A.J., Wallwork, M.D., Joachimski, M.M., Martin, L., Evans, N.J., Laming, B., McDonald, B.J., 2017. Digesting the data - effects of predator ingestion on the oxygen isotopic signature of micro-mammal teeth. Quat. Sci. Rev. 176, 71e84. https://doi.org/10.1016/j.quascirev.2017.10.004.

Bernard, A., Daux, V., Lécuyer, C., Brugal, J., Genty, D., Wainer, K., Gardien, V., Fourel, F., Jaubert, J., 2009. Pleistocene seasonal temperature variations recorded in the $\delta^{18}O$ of Bison priscus teeth. Earth Planet. Sci. Lett. 283, 133e143. https://doi.org/10.1016/j.epsl.2009.04.005.

Blain, H.-A., Bailon, S., Cuenca-Bescós, G., Arsuaga, J.L., Bermúdez de Castro, J.M., Carbonell, E., 2009. Long-term climate record inferred from early-middle Pleistocene amphibian and squamate reptile assemblages at the Gran Dolina Cave, Atapuerca, Spain. J. Hum. Evol. 56, 55e65. https://doi.org/10.1016/j.jhevol.2008.08.020.

Blain, H.A., Lozano-Fernández, I., Agustí, J., Bailon, S., Menéndez Granda, L., Espígares Ortiz, M.P., Ros-Montoya, S., Jiménez Arenas, J.M., Toro-Moyano, I., Martínez-Navarro, B., Sala, R., 2016. Refining upon the climatic background of the early Pleistocene hominid settlement in western Europe: Barranco León and Fuente Nueva-3 (Guadix-Baza basin, SE Spain). Quat. Sci. Rev. 144, 132e144. https://doi.org/10.1016/j.quascirev.2016.05.020.

Blake, R.E., Neil, R.O., Garcia, G.A., 1997. Oxygen isotope systematics of biologically mediated reactions of phosphate: I. Microbial degradation of organophosphorus compounds. Geochim. Cosmochim. Acta 61, 4411e4422.

Blumenthal, S.A., Cerling, T.E., Chritz, K.L., Bromage, T.G., Kozdon, R., Valley, J.W., 2014. Stable isotope time-series in mammalian teeth: in situ $\delta^{18}O$ from the innermost enamel layer. Geochim. Cosmochim. Acta 124, 223e236. https://doi.org/10.1016/j.gca.2013.09.032.

Bowen, G.J., 2017. The Online Isotopes in Precipitation Calculator, Version 3.1 (4/2017). http://waterisotopes.org.

Clementz, M.T., 2012. New insight from old bones: stable isotope analysis of fossil mammals. J. Mammal. 93, 368e380. https://doi.org/10.1644/11-MAMM-S-179.1.

Climate-Data.org, 2018. https://es.climate-data.org/.

Coady, J.M., Toto, P.D., Santangelo, M.V., 1967. Histology of the mouse incisor. J. Dent. Res. 46, 384e388.

Crowson, R.A., Showers, W.J., Wright, E.K., Hoering, T.C., 1991. Preparation of phosphate samples for oxygen isotope analysis. Anal. Chem. 63, 2397e2400. https://doi.org/10.1016/0031-0182(93)90085-W.

D'Angela, D., Longinelli, A., 1990. Oxygen isotopes in living mammal's bone phosphate: further results. Chem. Geol. 86, 75e82.

Dansgaard, W., 1964. Stable isotopes in precipitation. Tellus XVI, 436e468.

Daux, V., Lécuyer, C., Adam, F., Martineau, F., Vimeux, F., 2005. Oxygen isotope composition of human teeth and the record of climate changes in France (Lorraine) during the last 1,700 years. Clim. Change 70, 445e464. https://doi.org/10.1007/s10584-005-5385-6.

Delibes, M., Brunet-Lecomte, P., Mánez, M., 1983. Datos sobre la alimentación de la lechuza común (Tyto alba), el búho chico (Asio otus) y el mochuelo (Athene noctua) en una misma localidad de Castilla la Vieja. Ardeola 30, 57e63.

Fernández-García, M., López-García, J.M., Lorenzo, C., 2016. Palaeoecological implications of rodents as proxies for the Late PleistoceneeHolocene environmental and climatic changes in northeastern Iberia. Comptes Rendus Palevol 15, 707e719. https://doi.org/10.1016/j.crpv.2015.08.005.

Fletcher, W.J., Sánchez Goñi, M.F., Allen, J.R.M., Cheddadi, R., Combourieu-Nebout, N., Huntley, B., Lawson, I., Londeix, L., Magri, D., Margari, V., Müller, U.C., Naughton, F., Novenko, E., Roucoux, K., Tzedakis, P.C., 2010. Millennial-scale variability during the last glacial in vegetation records from Europe. Quat. Sci. Rev. 29, 2839e2864. https://doi.org/10.1016/j.quascirev.2009.11.015.

Fons, R., Saint Girons, M.C., 1993. Le cycle sexuel chez le mulot sylvestre, Apodemus sylvaticus (L., 1758), (Muridae) en region mediterraneenne. Z. Säugetierkd. 58, 38e47.

Font-Tullot, I., 2000. Climatología de España y Portugal. Universidad de Salamanca, Salamanca.

Fourel, F., Martineau, F., Lécuyer, C., Kupka, H.J., Lange, L., Ojeimi, C., Seed, M., 2011. $^{18}O/^{16}O$ ratio measurements of inorganic and organic materials by elemental analysisepyrolysiseisotope ratio mass spectrometry continuous-flow techniques. Rapid Commun. Mass Spectrom. 25, 2691e2696. https://doi.org/10.1002/rcm.5056.

Freudenthal, M., García-Alix, A., Rios, M., Ruiz-Sánchez, F., Martín-Suárez, E., Delgado, A., 2014. Review of paleo-humidity parameters in fossil rodents (Mammalia): isotopic vs. tooth morphology approach. Palaeogeogr. Palaeoclimatol. Palaeoecol. 395, 122e130. https://doi.org/10.1016/j.palaeo.2013.12.023.

Fricke, H.C., O'Neil, O., 1999. The correlation between 18O/16O ratios of meteoric water and surface temperature: its use in investigating terrestrial climate change over geologic time. Earth Planet. Sci. Lett. 170, 181e196. https://doi.org/10.1016/s0012-821x(99)00105-3.

García-Alix, A., 2015. A multiproxy approach for the reconstruction of ancient continental environments. The case of the MioePliocene deposits of the Granada Basin (southern Iberian Peninsula). Glob. Planet. Change 131, 1e10. https://doi.org/10.1016/j.gloplacha.2015.04.005.

Gat, J.R., 1980. The relationship between surface and subsurface waters: water quality aspects in areas of low precipitation. Hydrol. Sci. des Sci. Hydrol. 25, 257e267.

Gat, J.R., Carmi, I., 1970. Evolution of the Isotopic Composition of Atmospheric Waters im the Mediterranean Sea Area. J. Geophys. Res. 75, 3039e3048.

Gat, J.R., Klein, B., Kushnir, Y., Roether, W., Wernli, H., Yam, R., Shemesh, A., Klein, B., Kushnir, Y., Roether, W., Wernli, H., Yam, R., Shemesh, A., 2003. Isotope composition of air moisture over the Mediterranean Sea: an index of the air-sea interaction pattern. Chem. Phys. Meteorol. 55, 953e965. https://doi.org/10.3402/tellusb.v55i5.16395.

Gehler, A., Tütken, T., Pack, A., 2012. Oxygen and carbon isotope variations in a modern rodent community - implications for palaeoenvironmental reconstructions. PLoS One 7, 16e27. https://doi.org/10.1371/journal.pone.0049531.

Gehler, A., Tütken, T., Pack, A., 2011. Triple oxygen isotope analysis of bioapatite as tracer for diagenetic alteration of bones and teeth. Palaeogeogr. Palaeoclimatol. Palaeoecol. 310, 84e91. https://doi.org/10.1016/j.palaeo.2011.04.014.

Grimes, S.T., Collinson, M.E., Hooker, J.J., Mattey, D.P., 2008. Is small beautiful? A review of the advantages and limitations of using small mammal teeth and the direct laser fluorination analysis technique in the isotope reconstruction of past continental climate change. Palaeogeogr. Palaeoclimatol. Palaeoecol. 266, 39e50. https://doi.org/10.1016/j.palaeo.2008.03.014.

Grimes, S.T., Mattey, D.P., Hooker, J.J., Collinson, M.E., 2003. Palaeogene palaeoclimate reconstruction using oxygen isotopes from land and freshwater organisms: the use of multiple palaeoproxies. Geochim. Cosmochim. Acta 67, 4033e4047. https://doi.org/10.1016/S0016-7037(00)00173-X.

Hammer, Ø., Harper, D.A.T., Ryan, P.D., 2001. Paleontological statistics software package for education and data analysis. Palaeontol. Electron. 4, 9e18. https://doi.org/10.1016/j.bcp.2008.05.025.

Harrison, S.P., Sanchez Goñi, M.F., 2010. Global patterns of vegetation response to millennial-scale variability and rapid climate change during the last glacial period. Quat. Sci. Rev. 29, 2957e2980. https://doi.org/10.1016/j.quascirev.2010.07.016.

Hartman, G., Hovers, E., Hublin, J.-J., Richards, M., 2015. Isotopic evidence for Last Glacial climatic impacts on Neanderthal gazelle hunting territories at Amud Cave, Israel. J. Hum. Evol. 84, 71e82. https://doi.org/10.1016/j.jhevol.2015.03.008.

Héran, M.A., Lécuyer, C., Legendre, S., 2010. Cenozoic long-term terrestrial climatic evolution in Germany tracked by $\delta^{18}O$ of rodent tooth phosphate. Palaeogeogr. Palaeoclimatol. Palaeoecol. 285, 331e342. https://doi.org/10.1016/j.palaeo.2009.11.030.

Hernández Fernández, M., 2001. Bioclimatic discriminant capacity of terrestrial mammal faunas. Glob. Ecol. Biogeogr. 10, 189e204. https://doi.org/10.1046/j.1466-822x.2001.00218.x.

Hernández Fernández, M., Álvarez Sierra, M.Á., Peláez-Campomanes, P., 2007. Bioclimatic analysis of rodent palaeofaunas reveals severe climatic changes in Southwestern Europe during the Plio-Pleistocene. Palaeogeogr. Palaeoclimatol. Palaeoecol. 251, 500e526. https://doi.org/10.1016/j.palaeo.2007.04.015.

Hewitt, G.M., 2000. The genetic legacy of the Quarternary ice ages. Nature 405, 907e913. https://doi.org/10.1038/35016000.

Hillson, S., 2005. Teeth. Cambridge University Press, New York.

Hut, G., 1987. Consultants' Group Meeting on Stable Isotope Reference Samples for Geochemical and Hydrological Investigations, 16-18 Sep. 1985, Report to the Director General. International Atomic Energy Agency, Vienna.

IAEA/WMO, 2018. Global Network of Isotopes in Precipitation. The GNIP Database. Accessible at WISER (Water Isotope System for Data Analysis, Visualization and Electronic Retrieval). https://nucleus.iaea.org/wiser.

IUCN, 2018. The IUCN Red List of Threatened Species. Version 2017-3. www.iucnredlist.org.

Jeffrey, A., Denys, C., Stoetzel, E., Lee-Thorp, J.A., 2015. Influences on the stable oxygen and carbon isotopes in gerbillid rodent teeth in semi-arid and arid environments: implications for past climate and environmental reconstruction. Earth Planet. Sci. Lett. 428, 84e96. https://doi.org/10.1016/j.epsl.2015.07.012.

Klevezal, G.A., 2010. Dynamics of incisor growth and daily increments on the incisor surface in three species of small rodents. Biol. Butll. 37, 836e845. https://doi.org/10.1134/S1062359010080078.

Klevezal, G.A., Ek, M.P.U.C., Sukhovskaja, L.I., 1990. Incisor growth in voles. Acta Theriol. (Warsz). 35, 331e344.

Kolodny, Y., Luz, B., Navon, O., 1983. Oxygen isotope variations in phosphate of biogenic apatites, I. Fish bone apatite rechecking the rules of the game. Earth Planet. Sci. Lett. 64, 398e404.

Le Louarn, H., Quéré, J.P., 2003. Les Rongeurs de France. Faunistique et biologie. Editions d'Institut National de la Recherche Agronomique, Paris.

Lécuyer, C., 2014. Water on Earth. Iste Ltd and John Wiley & Sons Inc, London, UK and New York.

Lécuyer, C., 2004. Oxygen isotope analysis of phosphate. In: Groot, P.A. de (Ed.), Handbook of Stable Isotope Analytical Techniques. Elsevier B.V., pp. 482e499

Lécuyer, C., Atrops, F., Amiot, R., Angst, D., Daux, V., Flandrois, J., Fourel, F., Rey, K., Royer, A., Seris, M., Touzeau, A., Rousseau, D.D., 2018. Tsunami Sedimentary Deposits of Crete Records Climate during the 'Minoan Warming Period' (≥3350 Yr BP), pp. 1–16. The Holocene (in press). https://doi.org/10.1177/0959683617752840.

Lécuyer, C., Fourel, F., Martineau, F., Amiot, R., Bernard, A., Daux, V., Escarguel, G., Morrison, J., 2007. High-precision determination of $^{18}O/^{16}O$ ratios of silver phosphate by EA-pyrolysis-IRMS continuous flow technique. J. Mass Spectrom. 42, 36–41.

Lécuyer, C., Grandjean, P., O'Neil, J.R., Cappetta, H., Martineau, F., 1993. Thermal excursions in the ocean at the Cretaceous-Tertiary boundary (northern Morocco): $\delta^{18}O$ record of phosphatic fish debris. Palaeogeogr. Palaeoclimatol. Palaeoecol. 105, 235–243. https://doi.org/10.1016/0031-0182(93)90085-W.

Lécuyer, C., Grandjean, P., Sheppard, S.M.F., 1999. Oxygen isotope exchange between dissolved phosphate and water at temperatures ≤135°C: inorganic versus biological fractionations. Geochim. Cosmochim. Acta 63, 855–862. https://doi.org/10.1016/S0016-7037(99)00096-4.

Lee-Thorp, J.A., van der Merwe, N.J., 1991. Aspects of the chemistry of modern and fossil biological apatites. J. Archaeol. Sci. 18, 343–354. https://doi.org/10.1016/0305-4403(91)90070-6.

Leichliter, J., Sandberg, P., Passey, B., Codron, D., Avenant, N.L., Paine, O.C.C., Codron, J., de Ruiter, D., Sponheimer, M., 2017. Stable carbon isotope ecology of small mammals from the Sterkfontein Valley: implications for habitat reconstruction. Palaeogeogr. Palaeoclimatol. Palaeoecol. 485, 57–67. https://doi.org/10.1016/j.palaeo.2017.06.003.

Lindars, E.S., Grimes, S.T., Mattey, D.P., Collinson, M.E., Hooker, J.J., Jones, T.P., 2001. Phosphate $\delta^{18}O$ determination of modern rodent teeth by direct laser fluorination: an appraisal of methodology and potential application to palaeoclimate reconstruction. Geochim. Cosmochim. Acta 65, 2535–2548.

Longinelli, A., 1984. Oxygen isotopes in mammal bone phosphate: a new tool for paleohydrological and paleoclimatological research? Geochim. Cosmochim. Acta 48, 385–390. https://doi.org/10.1016/0016-7037(84)90259-X.

Longinelli, A., Nuti, S., 1973. Oxygen isotope measurements of phosphate from fish teeth and bones. Earth Planet. Sci. Lett. 20, 337–340. https://doi.org/10.1016/0012-821X(73)90007-1.

López-García, J.M., 2011. Los micromamíferos del Pleistoceno superior de la Península Ibérica. Evolución de la diversidad taxonómica y cambios paleoambientales y paleoclimáticos. Editorial Académica Española, Saarbrücken.

López-García, J.M., Blain, H.-A., Bennàsar, M., Euba, I., Barrals, S., Bischoff, J., López-Ortega, E., Saladié, P., Uzquiano, P., Vallverdú, J., 2012. A multiproxy reconstruction of the palaeoenvironment and palaeoclimate of the late Pleistocene in northeastern Iberia: cova dels Xaragalls, Vimbodí-Poblet, Paratge natural de Poblet, catalonia. Boreas 41, 235–249. https://doi.org/10.1111/j.1502-3885.2011.00234.x.

López-García, J.M., Blain, H.A., Bennàsar, M., Fernández-García, M., 2014. Environmental and climatic context of neanderthal occupation in southwestern Europe during MIS3 inferred from the small-vertebrate assemblages. Quat. Int. 326–327, 319–328.

Luz, B., Kolodny, Y., 1985. Oxygen isotope variations in phosphate of biogenic apatites, IV. Mammal teeth and bones. Earth Planet. Sci. Lett. 75, 29–36. https://doi.org/10.1016/0012-821X(85)90047-0.

Luz, B., Kolodny, Y., Horowitz, M., 1984. Fractionation of oxygen isotopes between mammalian. Geochim. Cosmochim. Acta 48, 1689–1693.

Luzi, E., 2018. Morphological and Morphometric Variations in Middle and Late Pleistocene in Microtus arvalis and Microtus agrestis Populations: Chronological Insight, Evolutionary Trends and Paleoclimatic and Palaeoenvironmental Inferences. Doctoral thesis. Universitat Rovira i Virgili, Tarragona, p. 316.

Manzanares, A., 2012. Aves rapaces de la Península Ibérica, Baleares y Canarias. Ediciones Omega, Barcelona.

Meteocat, 2018. http://www.meteo.cat/wpweb/climatologia/el-clima-ahir/el-clima-de-catalunya.

Mikkola, H., 1983. Owls of Europe. Buteo Books, Sussex.

Moreno, S., Kufner, M.B., 1988. Seasonal patterns in the wood mouse population in Mediterranean Scrubland. Acta Theriol. (Warsz). 33, 79–85.

Navarro, N., Montuire, S., Langlois, C., Martineau, F., 2004. Oxygen isotope compositions of phosphate from arvicoline teeth and Quaternary climatic changes, Gigny, French Jura. Quat. Res. 62, 172–182. https://doi.org/10.1016/j.yqres.2004.06.001.

Norrdahl, K., Korpima, E., 2002. Seasonal changes in the numerical responses of predators to cyclic vole populations. Ecography (Cop.) 25, 428–438.

Palomo, L.J., Gisbert, J., Blanco, C., 2007. Atlas y libro rojo de los mamíferos terrestres de España. Organismo Autónomo Parques Nacionales, Madrid.

Passey, B.H., Cerling, T.E., 2002. Tooth enamel mineralization in ungulates: implications for recovering a primary isotopic time-series. Geochim. Cosmochim. Acta 66, 3225–3234. https://doi.org/10.1016/S0016-7037(02)00933-X.

Peneycad, E., Candy, I., Schreve, D.C., 2019. Variability in the oxygen isotope compositions of modern rodent tooth carbonate: implications for palaeoclimate reconstructions. Palaeogeogr. Palaeoclimatol. Palaeoecol. 514, 695–705. https://doi.org/10.1016/J.PALAEO.2018.11.017.

Podlesak, D.W., Torregrossa, A., Ehleringer, J.R., Dearing, M.D., Passey, B.H., Cerling, T.E., 2008. Turnover of oxygen and hydrogen isotopes in the body water, CO_2, hair, and enamel of a small mammal. Geochim. Cosmochim. Acta 72, 19–35. https://doi.org/10.1016/j.gca.2007.10.003.

Pryor, A.J.E., Stevens, R.E., Connell, T.C.O., Lister, J.R., 2014. Quantification and propagation of errors when converting vertebrate biomineral oxygen isotope data to temperature for palaeoclimate reconstruction. Palaeogeogr. Palaeoclimatol. Palaeoecol. 412, 99–107. https://doi.org/10.1016/j.palaeo.2014.07.003.

R Core Team, 2017. R: A Language and Environment for Statistical Computing. R Foundation for Statistical Computing, Vienna, Austria. https://www.r-project.org/.

Rosário, I.T., Mathias, M.L., 2004. Annual weight variation and reproductive cycle of the wood mouse (Apodemus sylvaticus) in a Mediterranean environment. Mammalia 68, 133–140.

Royer, A., Lécuyer, C., Montuire, S., Amiot, R., Legendre, S., Cuenca-Bescós, G., Jeannet, M., Martineau, F., 2013a. What does the oxygen isotope composition of rodent teeth record? Earth Planet. Sci. Lett. 361, 258–271. https://doi.org/10.1016/j.epsl.2012.09.058.

Royer, A., Lécuyer, C., Montuire, S., Escarguel, G., Fourel, F., Mann, A., Maureille, B., 2013b. Late Pleistocene (MIS 3-4) climate inferred from micromammal communities and $\delta^{18}O$ of rodents from Les Pradelles, France. Quat. Res. 80, 113–124. https://doi.org/10.1016/j.yqres.2013.03.007.

Royer, A., Lécuyer, C., Montuire, S., Primault, J., Fourel, F., Jeannet, M., 2014. Summer air temperature, reconstructions from the last glacial stage based on rodents from the site Taillis-des-Coteaux (Vienne), Western France. Quat. Res. 82, 420–429. https://doi.org/10.1016/j.yqres.2014.06.006.

Rozanski, K., Araguás-Araguás, L., Gonfiantini, R., 1993. Isotopic patterns in modern global precipitation. In: Swart, P.K., Lohman, K.C., McKenzie, J., Savin, S. (Eds.), Climate Change in Continental Isotopic Records. Washington, pp. 1–36. https://doi.org/10.1029/GM078p0001.

Salamolard, M., Butet, A., Leroux, A., Bretagnolle, V., 2000. Responses of an avian predator to variations in prey density at a temperature latitude. Ecology 81, 2428–2441.

Sans-Coma, V., Gosalbez, J., 1976. Sobre la reproducción de Apodemus sylvaticus L, 1758 en el nordeste ibérico. Misc. Zool. III, 227–233.

Sánchez-González, B., Navarro-Castilla, A., Hernández, M.C., Barja, I., 2016. Ratón de campo – Apodemus sylvaticus. In: Salvador, A., Barja, I. (Eds.), Enciclopedia Virtual de los Vertebrados Españoles. Museo Nacional de Ciencias Naturales, Madrid. http://www.vertebradosibericos.org/.

Schrag, D.P., Adkins, J.F., Mcintyre, K., Alexander, J.L., Hodell, A., Charles, C.D., Mcmanus, J.F., 2002. The oxygen isotopic composition of seawater during the Last Glacial Maximum. Quat. Sci. Rev. 21, 331–342.

Sekour, M., Beddiaf, R., Souttou, K., Denys, C., Doumandji, S., Guezoul, O., 2011. Variation saisonnière du régime alimentaire de la Chouette chevêche (Athene noctua) (Scopoli, 1769) dans l' extrême Sud-Est du Sahara algérien (Djanet , Algérie). Rev. d'Écol. (La Terre la Vie) 66, 79–91.

Skrzypek, G., Sadler, R., Wi, A., 2016. Reassessment of recommendations for processing mammal phosphate $\delta^{18}O$ data for paleotemperature reconstruction. Palaeogeogr. Palaeoclimatol. Palaeoecol. 446, 162–167. https://doi.org/10.1016/j.palaeo.2016.01.032.

Sommer, R.S., Nadachowski, A., 2006. Glacial refugia of mammals in Europe: evidence from fossil records. Mamm Rev. 36, 251–265. https://doi.org/10.1111/j.1365-2907.2006.00093.x.

Sundell, J., Huitu, O., Henttonen, H., Kaikusalos, A., Korpimäki, E., Pietiäinen, H., Saurola, P., Hanski, I., 2004. Large-scale spatial dynamics of vole populations in Finland revealed by the breeding success of vole-eating avian predators. J. Anim. Ecol. 73, 167–178.

Sunyer, P., Muñoz, A., Mazerolle, M.J., Bonal, R., Espelta, J.M., 2016. Wood mouse population dynamics: interplay among seed abundance seasonality, shrub cover and wild boar interference. Mamm. Biol. 81, 372–379. https://doi.org/10.1016/j.mambio.2016.03.001.

Uriarte, A., 2003. Historia del clima de la Tierra. Vitoria-Gasteiz: Servicio Central de Publicaciones del Gobierno Vasco.

Vallverdú, J., López-García, J.M., Blain, H.-A., Saladíe, P., Uzquiano, P., Bischoff, J., Vaquero, M., 2012. El Pleistocè de la cova dels Xaragalls. In: III Jornades Del Bosc de Poblet i Es Muntanyes de Prades, pp. 241–250.

von Grafenstein, U., Erlenkeuser, H., Müller, J., Trimborn, P., Alefs, J., 1996. A 200 year mid-European air temperature record preserved in lake sediments: an extension of the $\delta^{18}O_p$-air temperature relation into the past. Geochim. Cosmochim. Acta 60, 4025–4036.

Yalden, D.W., 2009. Dietary separation of owls in the peak district. Bird Study 32, 122–131. https://doi.org/10.1080/00063658509476867.

Zazzo, A., Lécuyer, C., Mariotti, A., 2004. Experimentally-controlled carbon and oxygen isotope exchange between bioapatites and water under inorganic and microbially-mediated conditions. Geochim. Cosmochim. Acta 68, 1–12. https://doi.org/10.1016/S0016-7037(03)00278-3.